

MHD turbulence in stars, discs, & galaxies

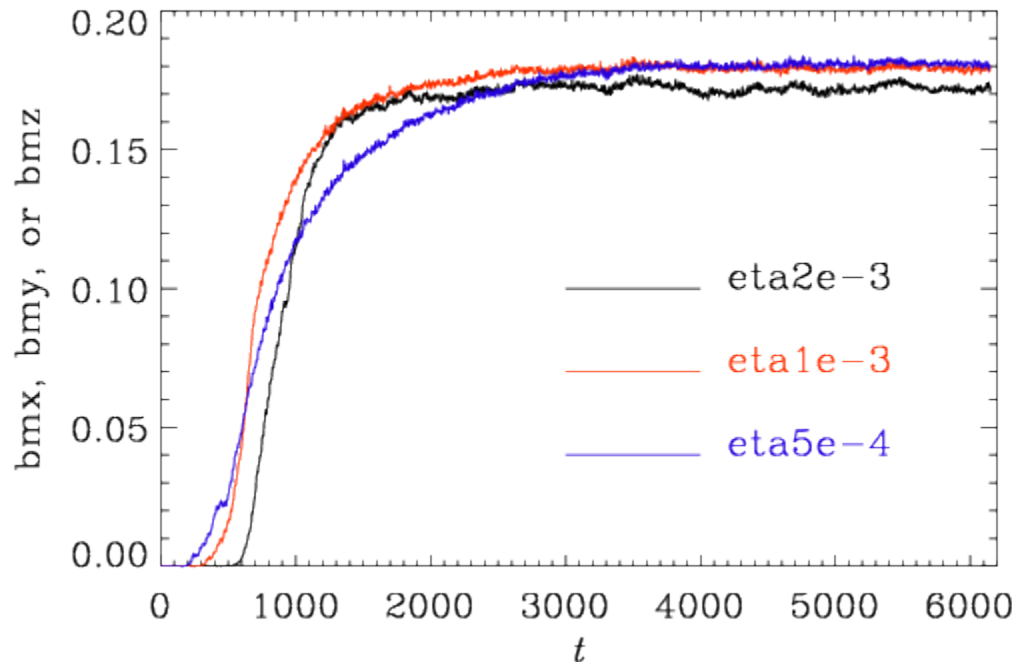
+SNR

Axel Brandenburg (Nordita, Stockholm)

(...just google for Pencil Code)

Comments on yesterday's exercise

- Saturation slower for smaller eta (\rightarrow fluxes)
- Higher resolution
 - Larger growth rate
 - Similar saturation
 - Theoretical prediction ok



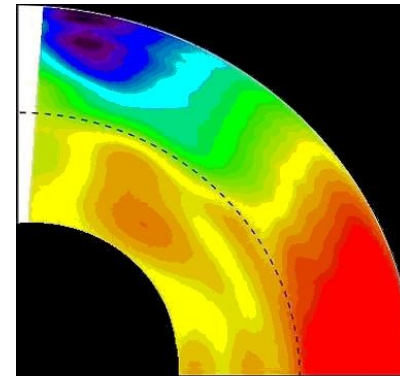
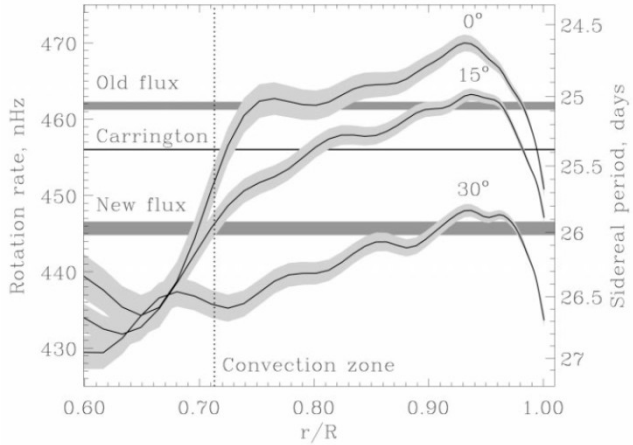
Results (all for nu=2e-2, force=0.07) :

Res	2e-3	lambda	tsat	ampl	brms	urms	bfrms	b2kf_k1	Run
16	2e-3	0.0272	850	0.0295	0.199	0.123	0.100	0.0311	helical-MHDturb
16	5e-4	0.0723	500	0.0335	0.211	0.123	0.106	0.0349	helical-MHDturb
64	5e-4	0.0326	530	0.0465	0.244	0.124	0.115	0.0414	helical-MHDturb-64
128	5e-4	0.0325	520	0.046	0.244	0.124	0.116	0.0423	helical-MHDturb-128

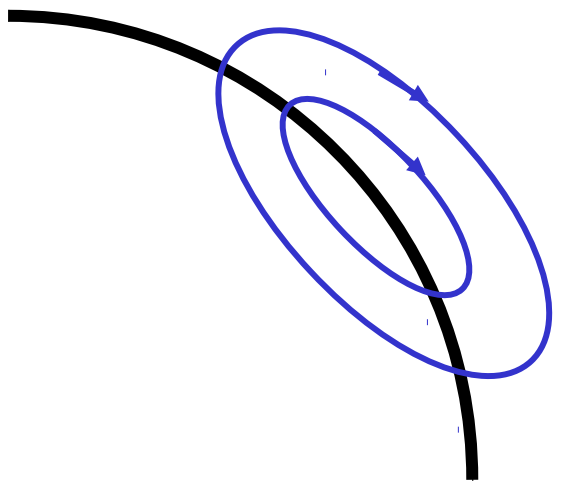
□

Simulations of the solar dynamo?

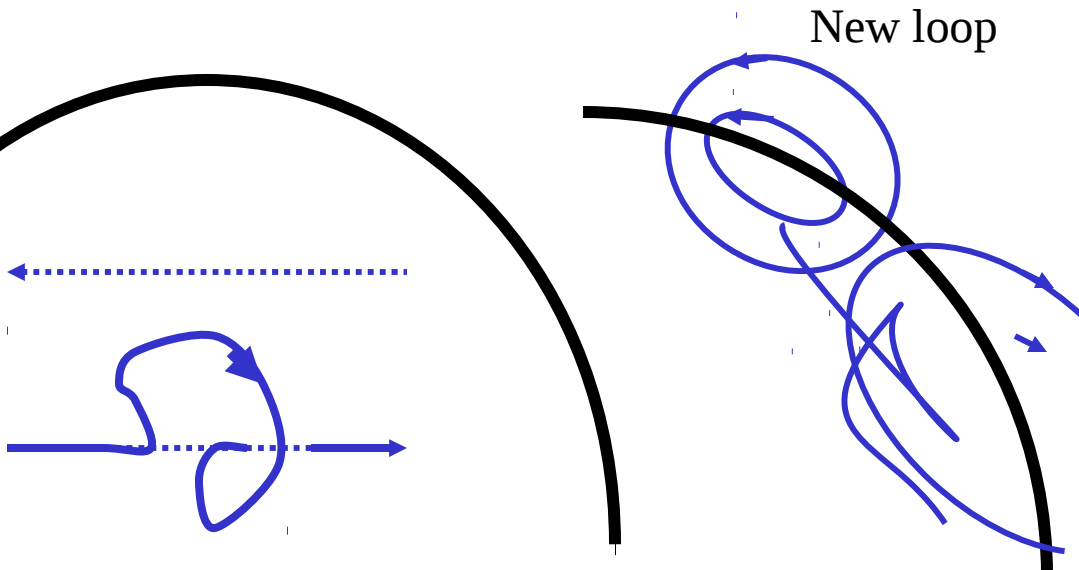
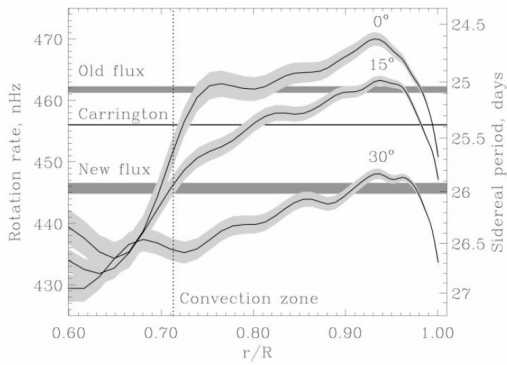
- Tremendous stratification
 - Not only density, also scale height change
- Near-surface shear layer (NSSL) not resolved
- Contours of Ω cylindrical, not spoke-like
- (i) R_m dependence (catastrophic quenching)
 - Field is bi-helical: to confirm for solar wind
- (ii) Location: bottom of CZ or distributed
 - Shaped by NSSL (Brandenburg 2005, ApJ 625, 539)
 - Formation of active regions near surface



Standard dynamo wave

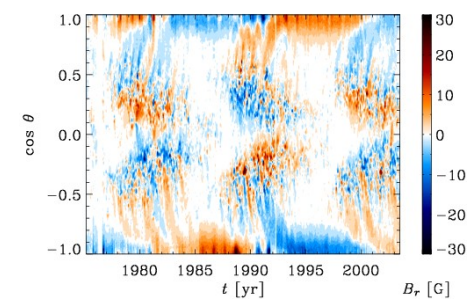
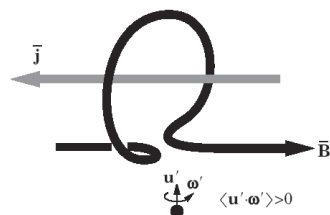


Differential rotation
(faster inside)

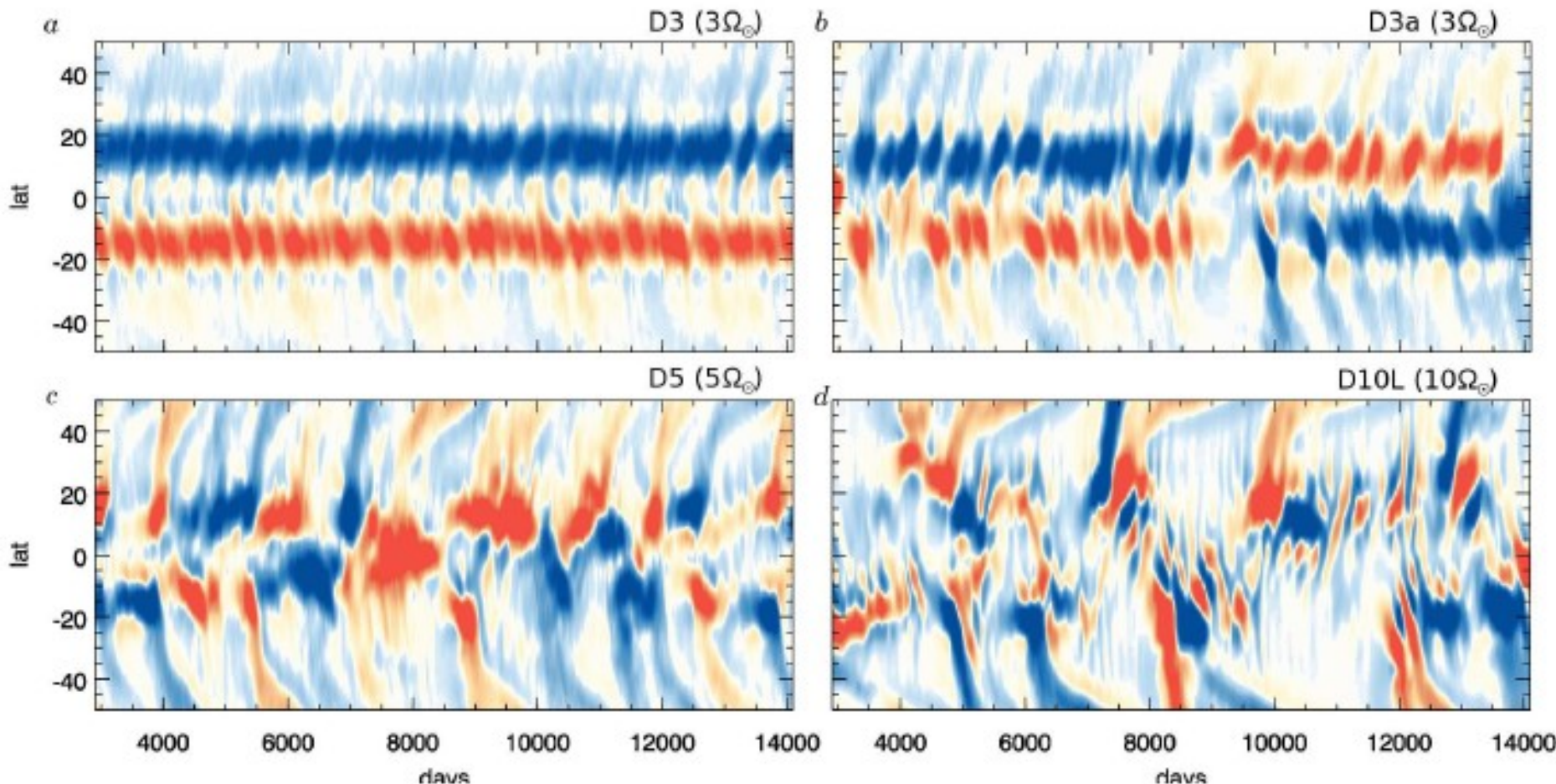


Cyclonic convection;
Buoyant flux tubes

→ α -effect



Brun, Brown, Browning, Miesch, Toomre

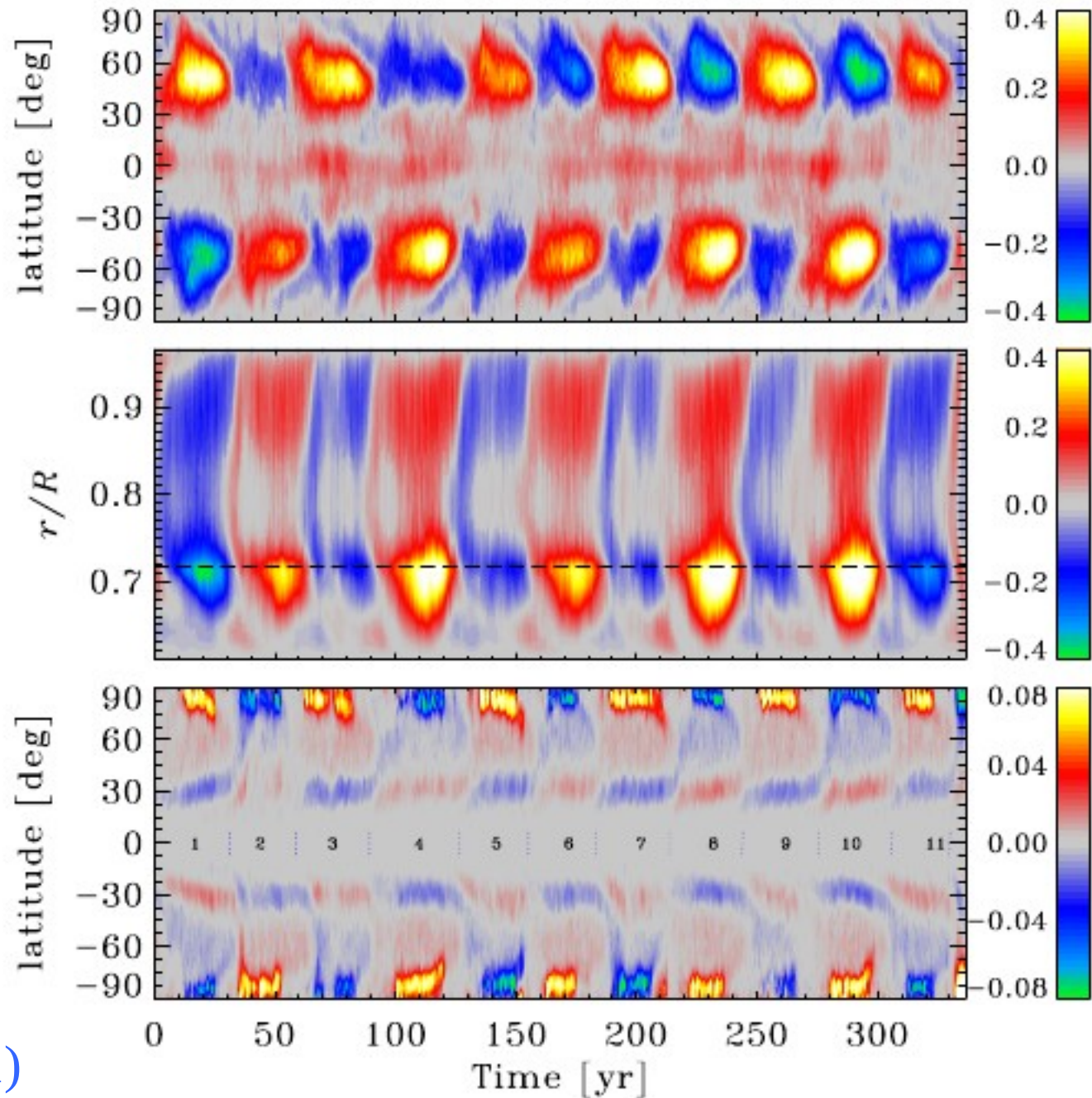


ASH code: anelastic
spherical harmonics

Brown et al. (2011)

*Ghizaru,
Charbonneau,
Racine, ...*

- Cycle now common!
- Activity from bottom of CZ
- but at high latitudes

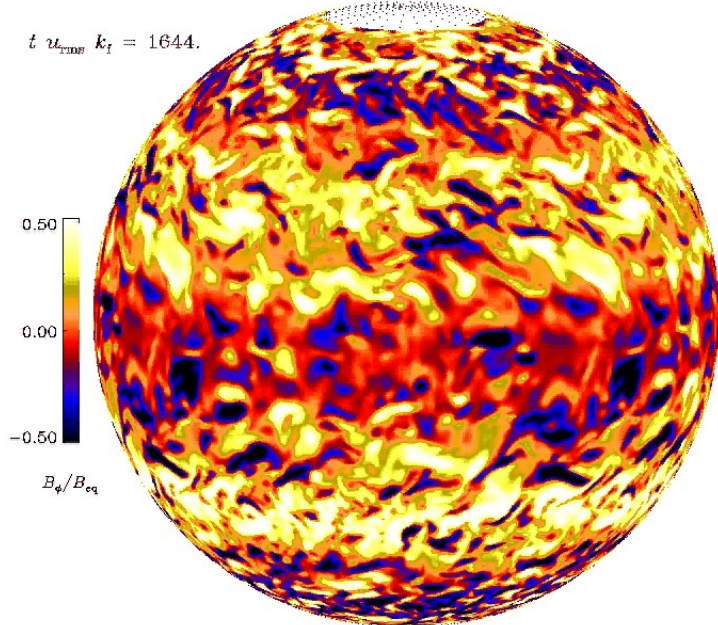
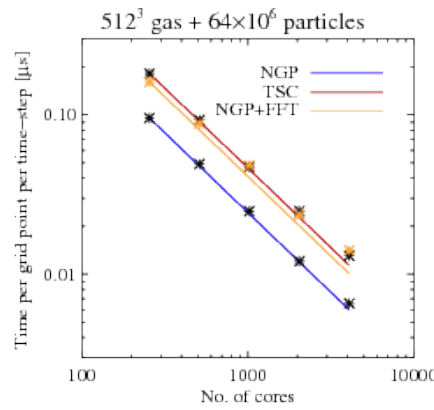
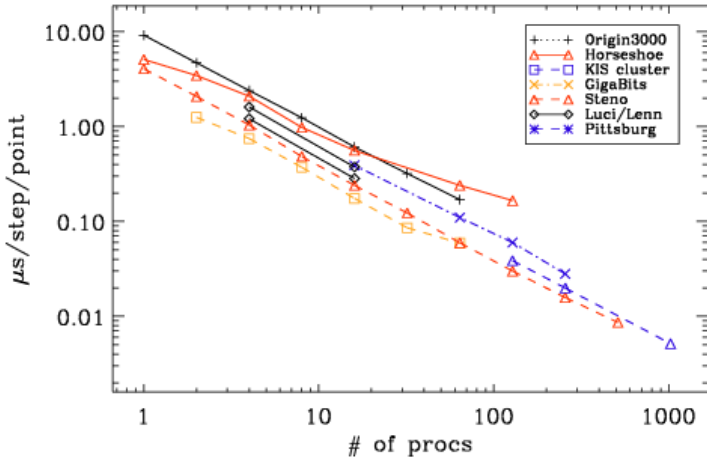


Racine et al. (2011)



Pencil code

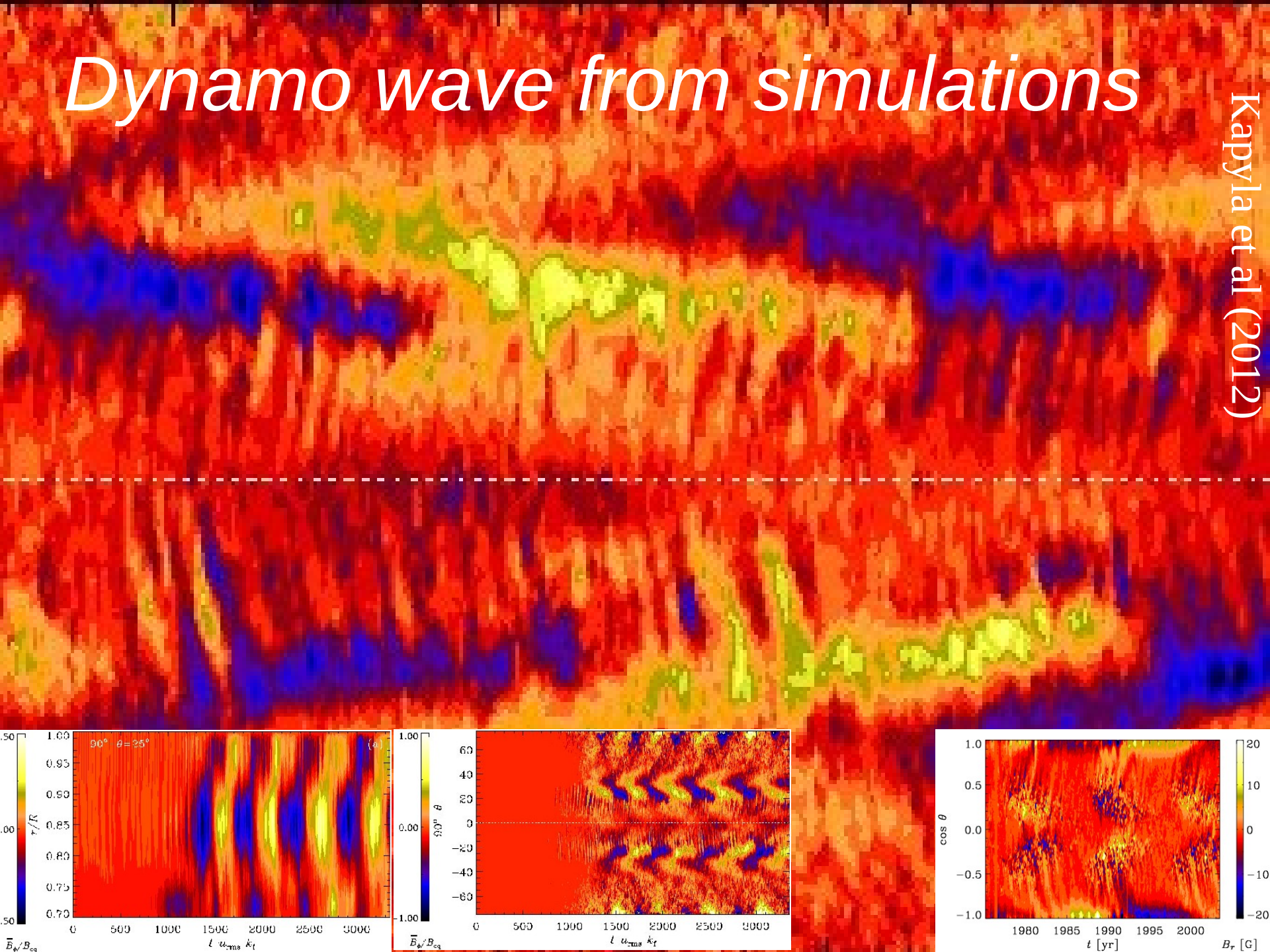
- Started in Sept. 2001 with Wolfgang Dobler
- High order (6th order in space, 3rd order in time)
- Cache & memory efficient
- MPI, can run PacxMPI (across countries!)
- Maintained/developed by ~80 people (SVN)
- Automatic validation (over night or any time)
- 0.0013 $\mu\text{s}/\text{pt}/\text{step}$ at 1024^3 , 2048 procs
- <http://pencil-code.googlecode.com>



- Isotropic turbulence
 - MHD, passive scl, CR
- Stratified layers
 - Convection, radiation
- Shearing box
 - MRI, dust, interstellar
 - Self-gravity
- Sphere embedded in box
 - Fully convective stars
 - geodynamo
- Other applications
 - Chemistry, combustion
 - Spherical coordinates

Dynamo wave from simulations

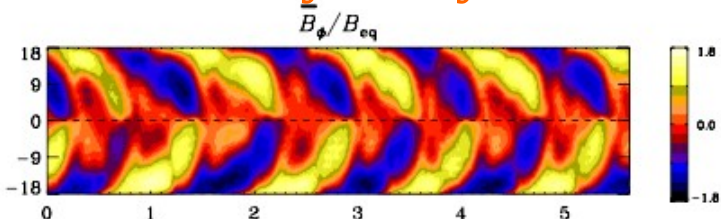
Kapyla et al (2012)



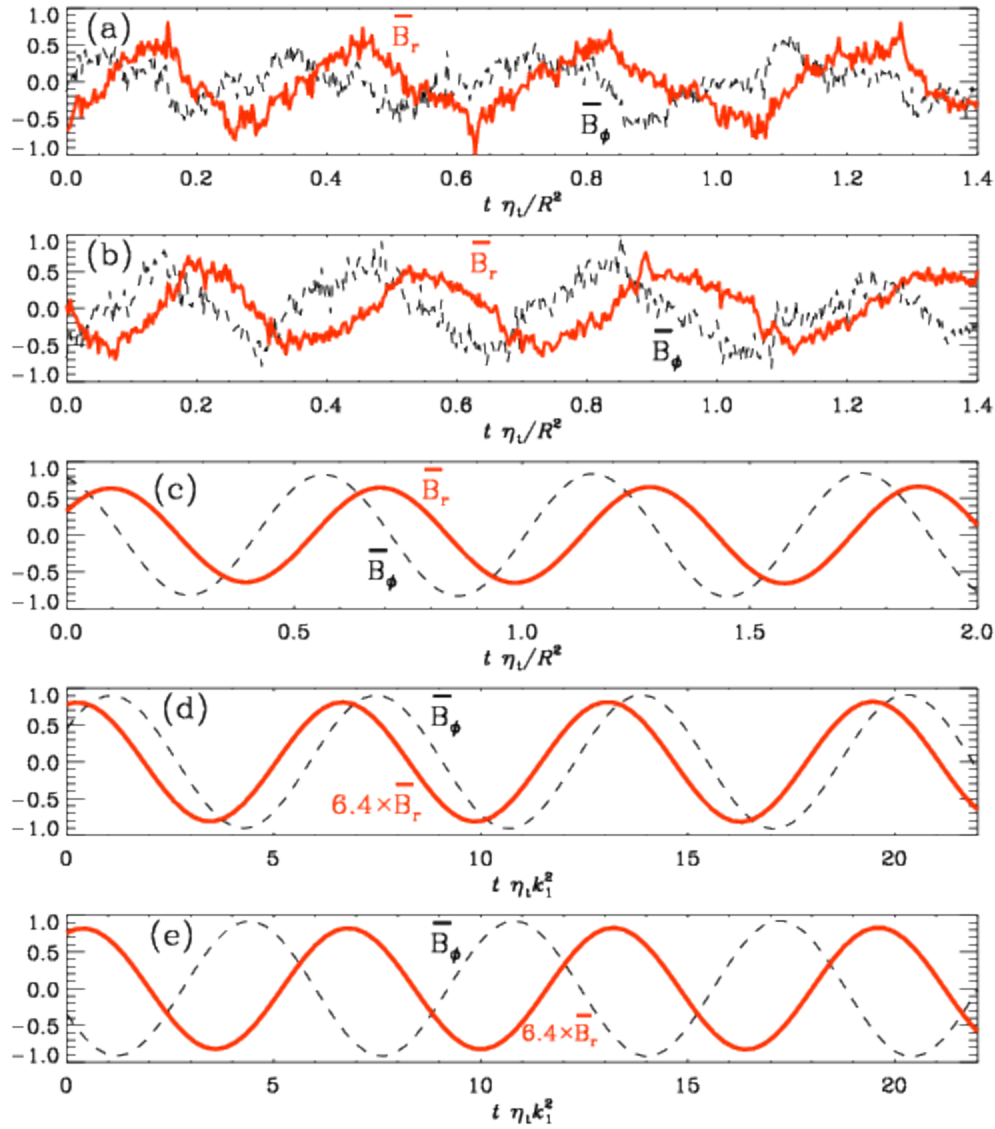
Type of dynamo?

- Use phase relation
- Closer to α^2 dynamo
- Wrong for $\alpha\Omega$ dyn.

Oscillatory α^2 dynamo



Mitra et al. (2010)



Calculate full α_{ij} and η_{ij} tensors

$$\frac{\partial \bar{\mathbf{A}}}{\partial t} = \bar{\mathbf{U}} \times \bar{\mathbf{B}} + \bar{\boldsymbol{\epsilon}} - \eta \bar{\mathbf{J}}$$

turbulent emf $\bar{\boldsymbol{\epsilon}} = \overline{\mathbf{u} \times \mathbf{b}}$

α effect and turbulent
magnetic diffusivity

$$\bar{\boldsymbol{\epsilon}}_j = \alpha_{ij} \bar{B}_j - \eta_{ij}^* \bar{J}_j$$

- Imposed-field method
 - Convection (Brandenburg et al. 1990)
- Correlation method
 - MRI accretion discs (Brandenburg & Sokoloff 2002)
 - Galactic turbulence (Kowal et al. 2005, 2006)
- Test field method
 - Stationary geodynamo (Schrinner et al. 2005, 2007)

Calculate full α_{ij} and η_{ij} tensors

$$\frac{\partial \mathbf{A}}{\partial t} = \mathbf{U} \times \mathbf{B} - \eta \mathbf{J} \quad \text{Original equation (uncurled)}$$

$$\frac{\partial \overline{\mathbf{A}}}{\partial t} = \overline{\mathbf{U}} \times \overline{\mathbf{B}} + \overline{\mathbf{u} \times \mathbf{b}} - \eta \overline{\mathbf{J}} \quad \text{Mean-field equation}$$

$$\frac{\partial \mathbf{a}}{\partial t} = \overline{\mathbf{U}} \times \mathbf{b} + \mathbf{u} \times \overline{\mathbf{B}} + \mathbf{u} \times \mathbf{b} - \overline{\mathbf{u} \times \mathbf{b}} - \eta \mathbf{j} \quad \text{fluctuations}$$

Response to arbitrary mean fields

$$\frac{\partial \mathbf{a}^{pq}}{\partial t} = \overline{\mathbf{U}} \times \mathbf{b}^{pq} + \mathbf{u} \times \overline{\mathbf{B}}^{pq} + \mathbf{u} \times \mathbf{b}^{pq} - \overline{\mathbf{u} \times \mathbf{b}^{pq}} - \eta \mathbf{j}^{pq}$$

Test fields

$$\bar{\mathbf{B}}^{11} = \begin{pmatrix} \cos kz \\ 0 \\ 0 \end{pmatrix}, \quad \bar{\mathbf{B}}^{21} = \begin{pmatrix} \sin kz \\ 0 \\ 0 \end{pmatrix}$$

$$\bar{\mathbf{B}}^{12} = \begin{pmatrix} 0 \\ \cos kz \\ 0 \end{pmatrix}, \quad \bar{\mathbf{B}}^{22} = \begin{pmatrix} 0 \\ \sin kz \\ 0 \end{pmatrix}$$

$$\bar{\mathcal{E}}_j^{pq} = \alpha_{ij} \bar{B}_j^{pq} + \eta_{ijk} \bar{B}_{j,k}^{pq}$$

Example:

$$\bar{\mathcal{E}}_1^{11} = \alpha_{11} \cos kz - \eta_{113} k \sin kz$$

$$\bar{\mathcal{E}}_1^{21} = \alpha_{11} \sin kz + \eta_{113} k \cos kz$$

$$\begin{pmatrix} \alpha_{11} \\ \eta_{113} k \end{pmatrix} = \begin{pmatrix} \cos kz & \sin kz \\ -\sin kz & \cos kz \end{pmatrix} \begin{pmatrix} \bar{\mathcal{E}}_1^{11} \\ \bar{\mathcal{E}}_1^{21} \end{pmatrix}$$

$$\begin{pmatrix} \eta_{11}^* & \eta_{12}^* \\ \eta_{21}^* & \eta_{22}^* \end{pmatrix} = \begin{pmatrix} \eta_{123} & -\eta_{113} \\ \eta_{223} & -\eta_{213} \end{pmatrix}$$

Validation: Roberts flow

$$U = u_{rms} \begin{pmatrix} -\cos k_x x \sin k_y y \\ +\sin k_x x \cos k_y y \\ \sqrt{2} \cos k_x x \cos k_y y \end{pmatrix}$$

$$\frac{\partial \mathbf{a}^{pq}}{\partial t} = \overline{\mathbf{U}} \times \mathbf{b}^{pq} + \mathbf{u} \times \overline{\mathbf{B}}^{pq} + \cancel{\mathbf{u} \times \mathbf{b}^{pq}} - \cancel{\mathbf{u} \times \mathbf{b}^{pq}} - \eta \mathbf{j}^{pq}$$

SOCA

$$k_x = k_y = k_f / \sqrt{2}$$

SOCA result

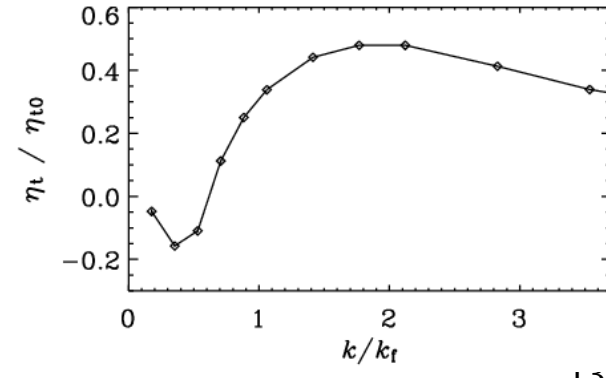
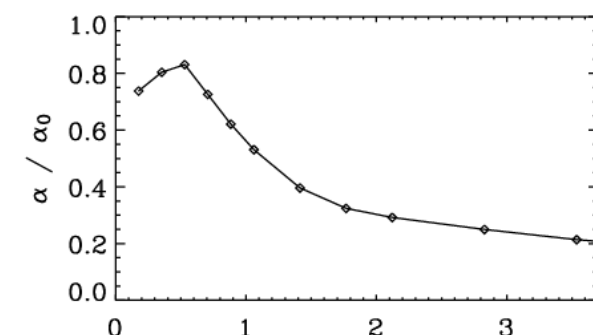
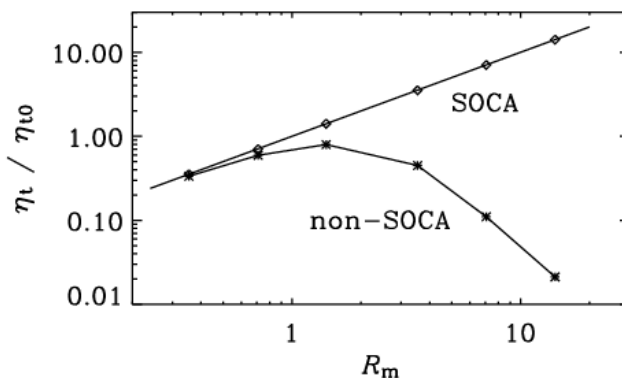
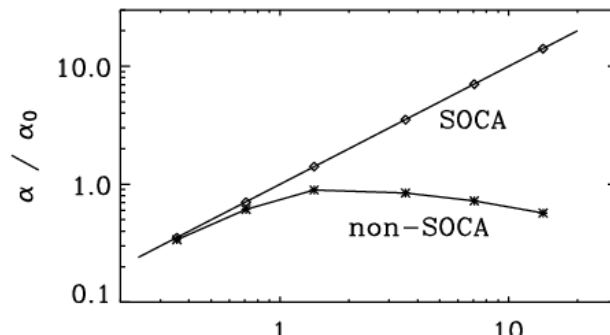
$$\alpha = -\frac{1}{3} R_m u_{rms}$$

$$\eta_t = \frac{1}{3} R_m u_{rms} k_f^{-1}$$

normalize

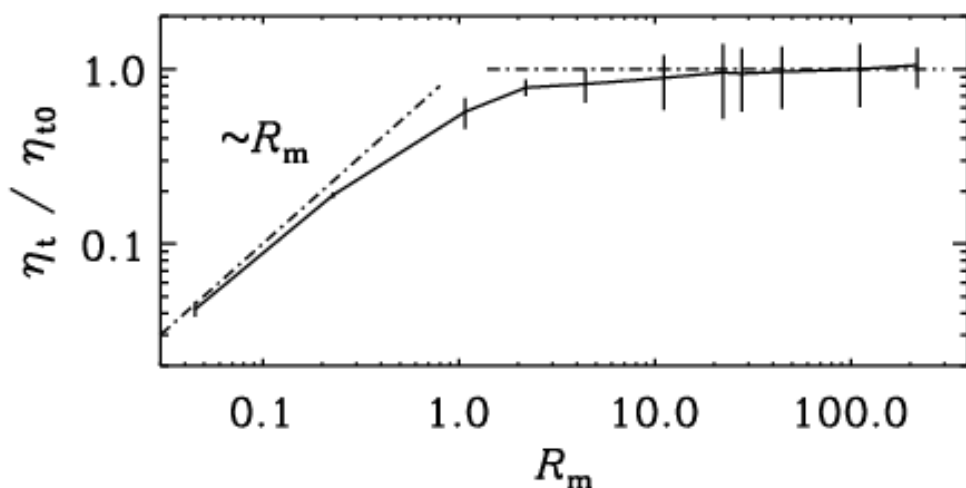
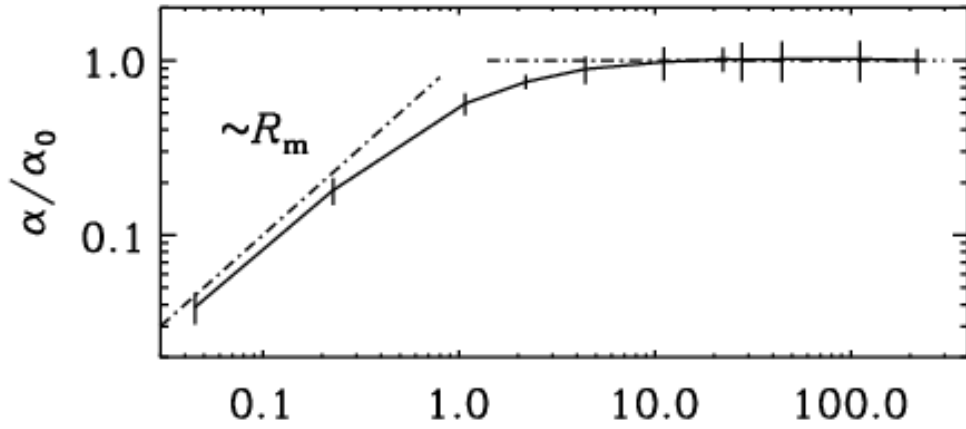
$$\alpha_0 = -\frac{1}{3} u_{rms}$$

$$\eta_{t0} = \frac{1}{3} u_{rms} k_f^{-1}$$



Test-field results for α and η_t

kinematic: independent of R_m (2...200)



$$\alpha_0 = -\frac{1}{3} \tau \langle \boldsymbol{\omega} \cdot \mathbf{u} \rangle$$

$$\eta_0 = \frac{1}{3} \tau \langle \mathbf{u}^2 \rangle$$

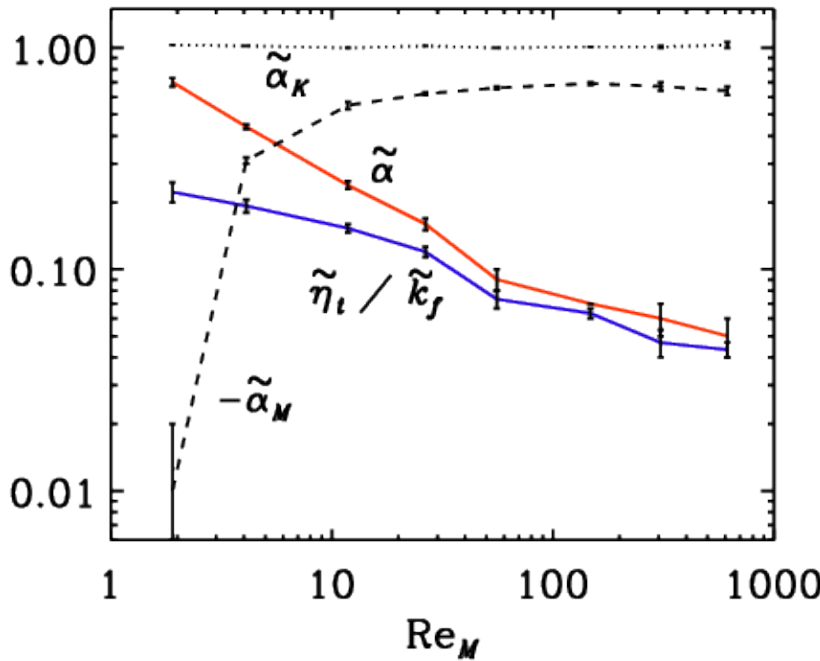
$$\tau = (u_{\text{rms}} k_f)^{-1}$$

$$\alpha_0 = -\frac{1}{3} u_{\text{rms}}$$

$$\eta_0 = \frac{1}{3} u_{\text{rms}} k_f^{-1}$$

Sur et al. (2008, MNRAS)

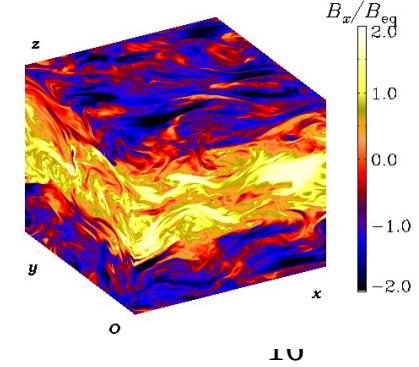
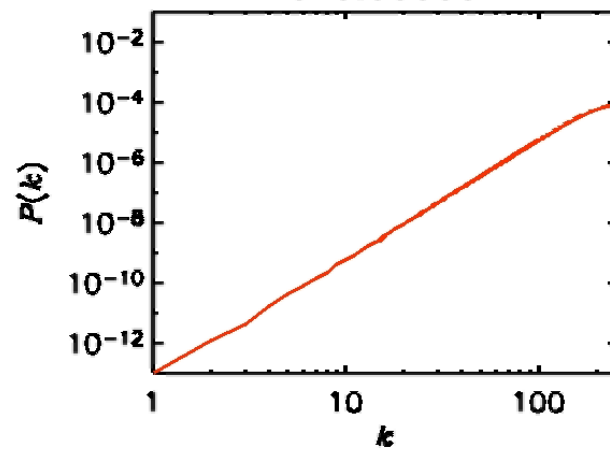
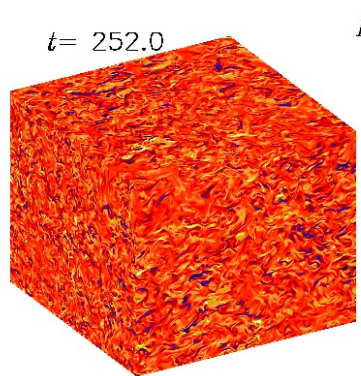
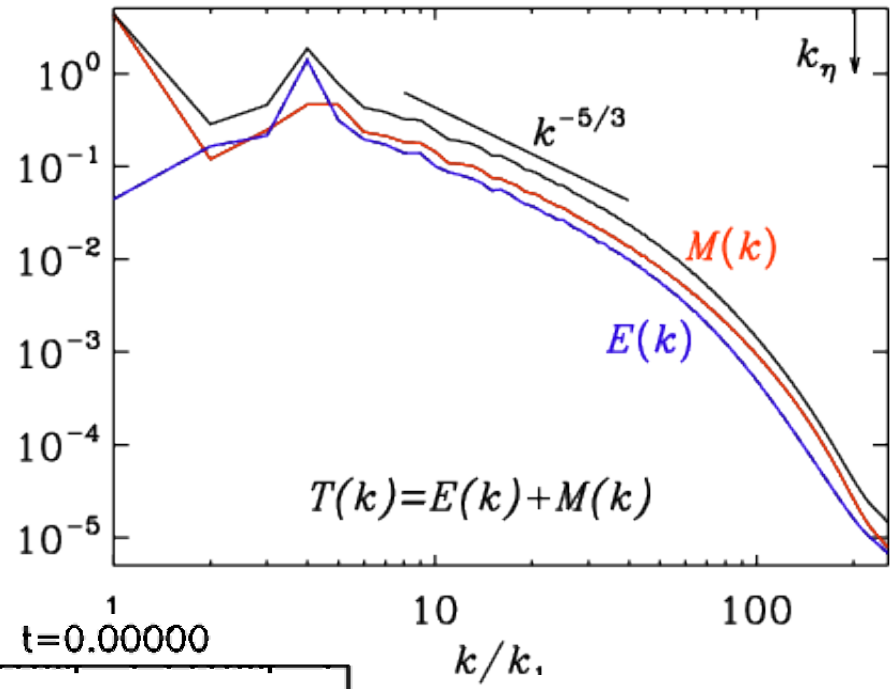
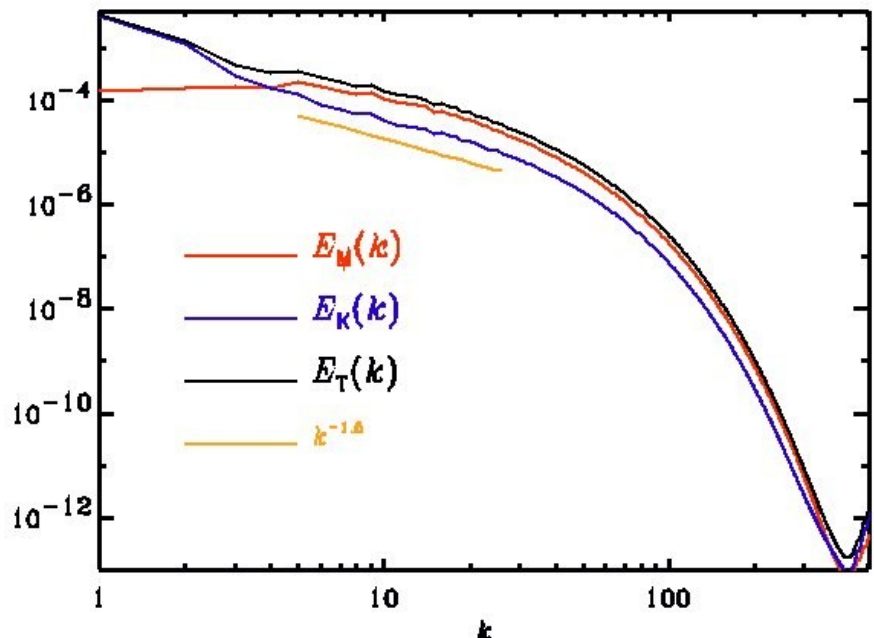
R_m dependence for $B \sim B_{eq}$



- (i) \square is small \rightarrow consistency
- (ii) \square_1 and \square_2 tend to cancel
- (iii) making \square small
- (iv) \square_2 small

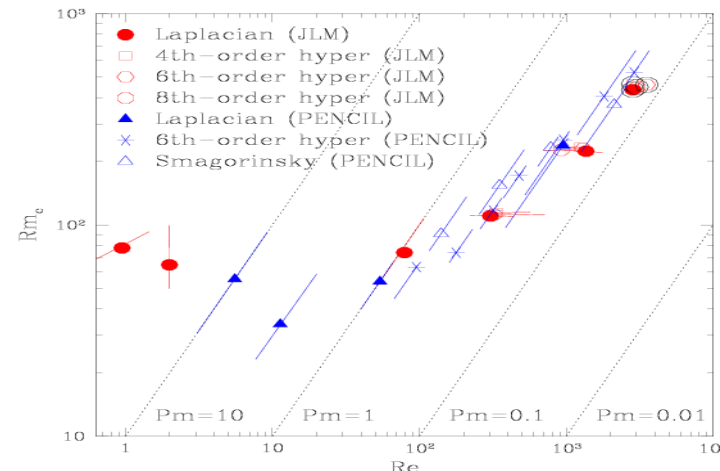
Run	Re_M	\tilde{B}^2	\tilde{b}^2	$\tilde{\alpha}$	$\tilde{\eta}_t$	$\tilde{\eta}$	λ	$-\tilde{\alpha}_2$	$-\tilde{\eta}_2$	$\tilde{\alpha}_{rms}$	$\tilde{\eta}_{rms}$	$+\tilde{\alpha}_K$	$-\tilde{\alpha}_M$	$\Delta\tilde{r}$
A	2	0.0	0.0	0.70 ± 0.03	0.67 ± 0.07	1.57	-0.14 ± 0.01	0.04 ± 0.05	-0.02 ± 0.06	0.09	0.12	1.03	0.01	150
B	4	0.9	0.4	0.44 ± 0.01	0.58 ± 0.04	0.73	0.00 ± 0.00	0.33 ± 0.02	-0.11 ± 0.03	0.10	0.21	1.02	0.31	422
C	12	1.7	0.7	0.24 ± 0.01	0.46 ± 0.02	0.25	0.00 ± 0.00	0.37 ± 0.02	-0.04 ± 0.01	0.09	0.16	1.00	0.55	601
D	30	1.9	0.8	0.16 ± 0.01	0.36 ± 0.02	0.11	-0.00 ± 0.01	0.37 ± 0.02	0.03 ± 0.03	0.07	0.14	1.02	0.62	350
E	60	2.0	0.8	0.09 ± 0.01	0.22 ± 0.02	0.05	0.00 ± 0.01	0.33 ± 0.01	0.05 ± 0.01	0.09	0.22	1.00	0.66	711
F	150	2.0	0.9	0.07 ± 0.00	0.19 ± 0.01	0.02	0.01 ± 0.01	0.24 ± 0.05	0.08 ± 0.01	0.07	0.16	1.01	0.69	225
G	300	1.8	0.9	0.06 ± 0.00	0.15 ± 0.00	0.01	0.01 ± 0.01	0.21 ± 0.02	0.05 ± 0.02	0.06	0.16	1.01	0.66	177
H	600	1.8	0.9	0.05 ± 0.01	0.13 ± 0.01	0.005	0.01 ± 0.04	0.14 ± 0.05	0.04 ± 0.01	0.05	0.10	1.03	0.64	44

Small-scale vs large-scale dynamo

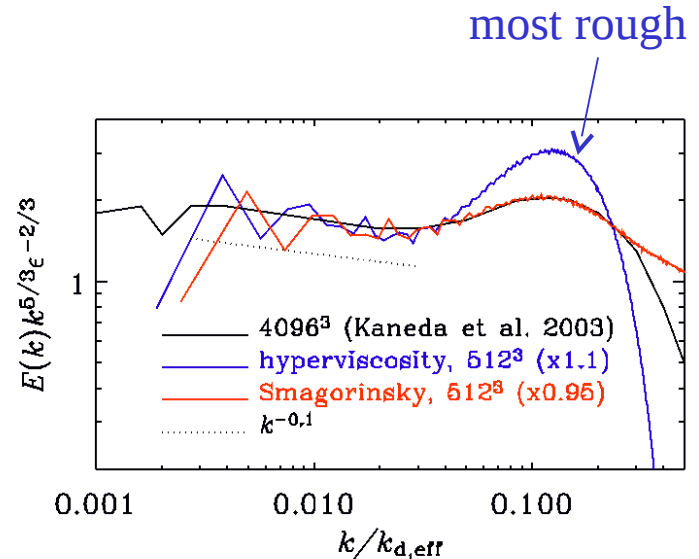
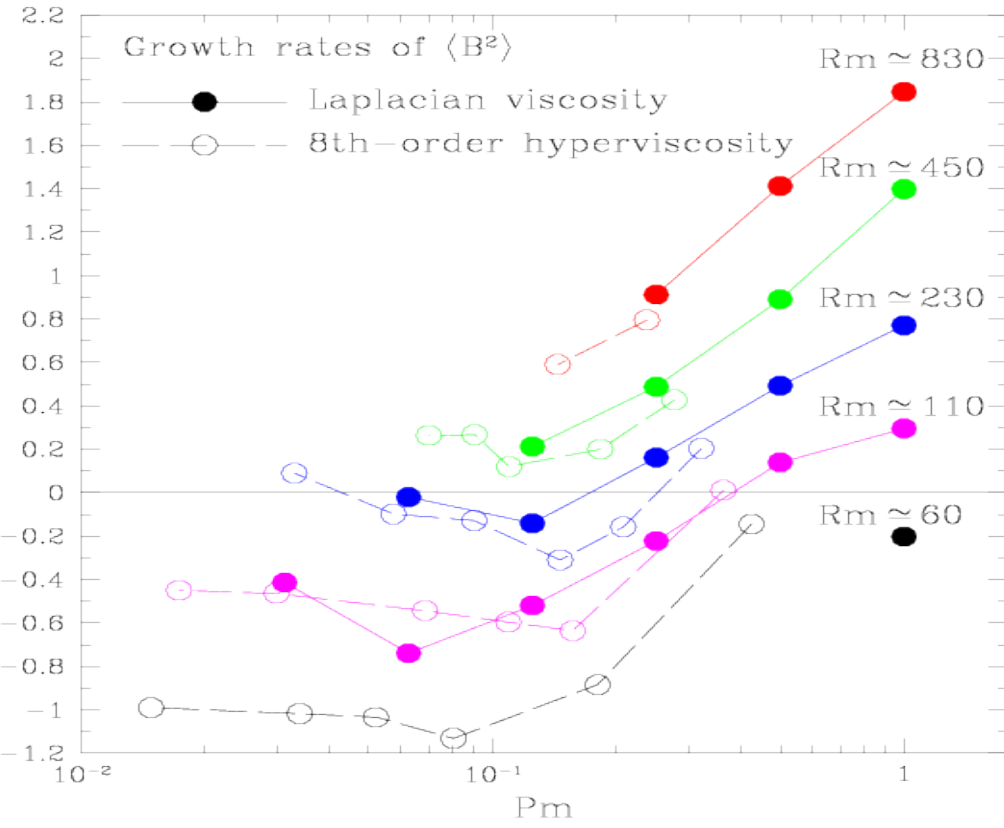


Low Pr_M issue

- Small-scale dynamo: $R_{m,crit} = 35-70$ for $Pr_M = 1$ (Novikov, Ruzmaikin, Sokoloff 1983)
- Leorat et al (1981): independent of Pr_M (EDQNM)
- Rogachevskii & Kleeorin (1997): $R_{m,crit} = 412$
- Boldyrev & Cattaneo (2004): relation to roughness
- Ponty et al.: (2005) · levels off at $Pr = 0.2$



Re-appearance at low Pr_M

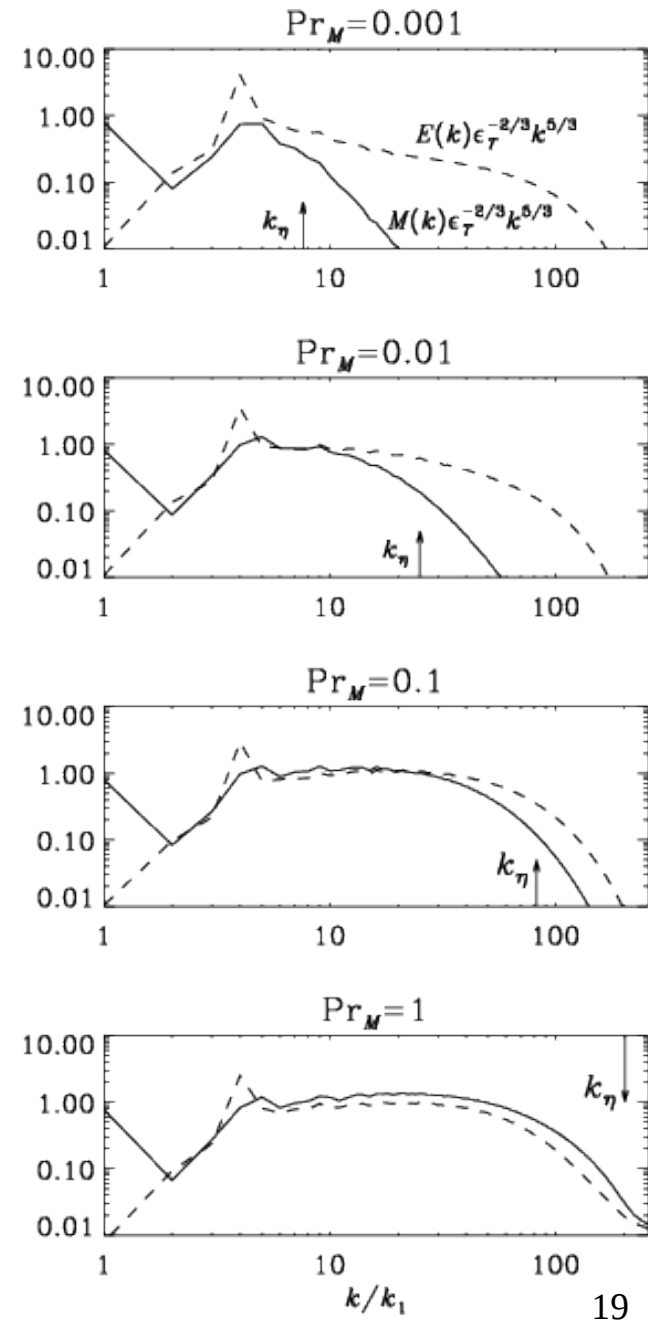
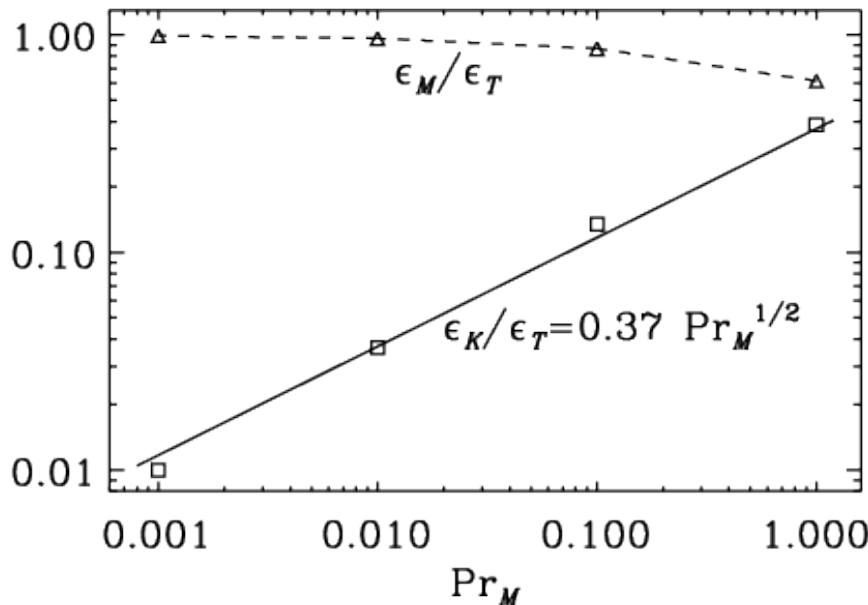


Gap between
0.05 and 0.2 ?

Iskakov et al (2005)

Low Pr_M dynamos with helicity do work

- Energy dissipation via Joule
- Viscous dissipation weak
- Can increase Re substantially!



Discs & magneto-rotational instability

Vertical field B_0

$$\dot{u}_x - 2\Omega u_y = B_{0z} b_x' \quad \Omega(r) \propto r^{-q}$$

$$\dot{u}_y + (2-q)\Omega u_x = B_{0z} b_y'$$

$$\dot{b}_x = B_{0z} u_x'$$

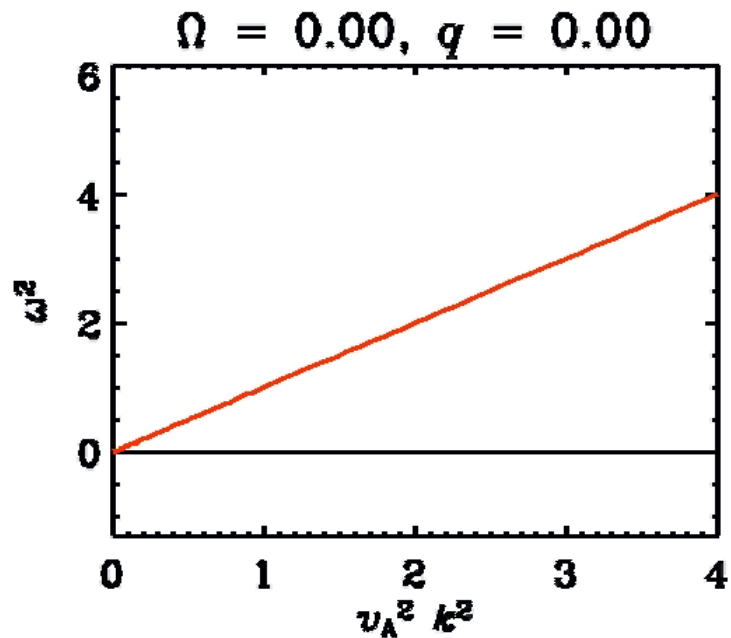
$$\dot{b}_y = B_{0z} u_y' - q\Omega b_x$$

Dispersion relation

$$\omega^4 - \omega^2 [2\omega_A^2 + 2(2-q)\Omega^2] + \omega_A^2 (\omega_A^2 - 2q\Omega^2) = 0$$

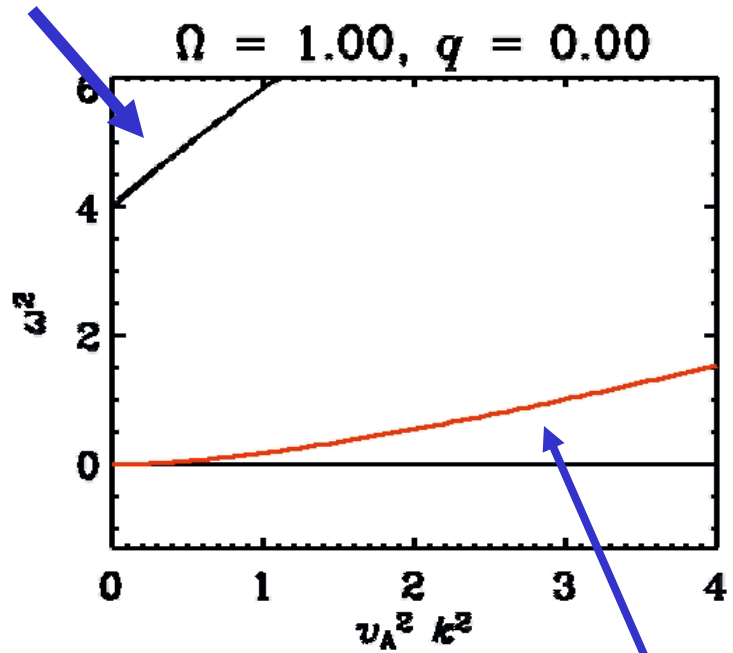
Alfven frequency: $\omega_A = v_A k$

Alfven and slow magnetosonic waves



Degeneracy lifted by q or $\Omega \neq 0$

Alfven

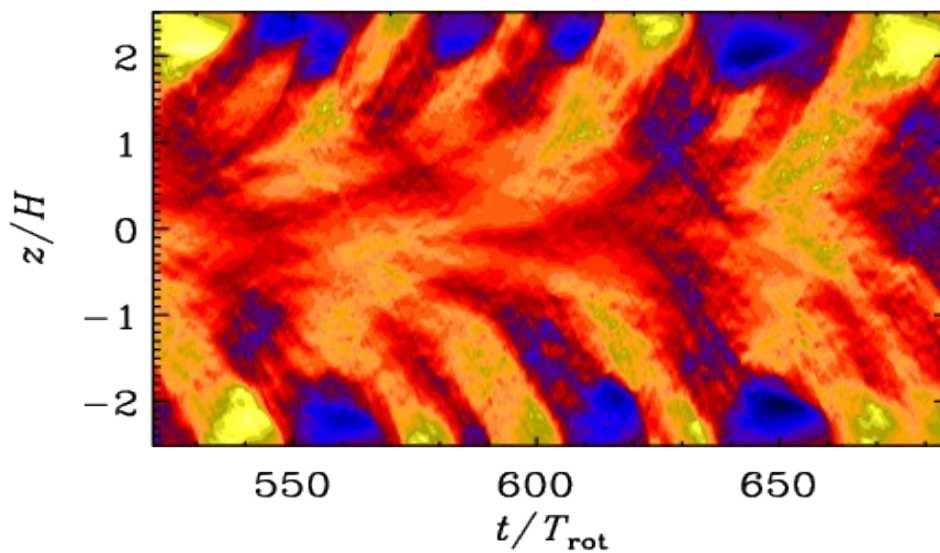
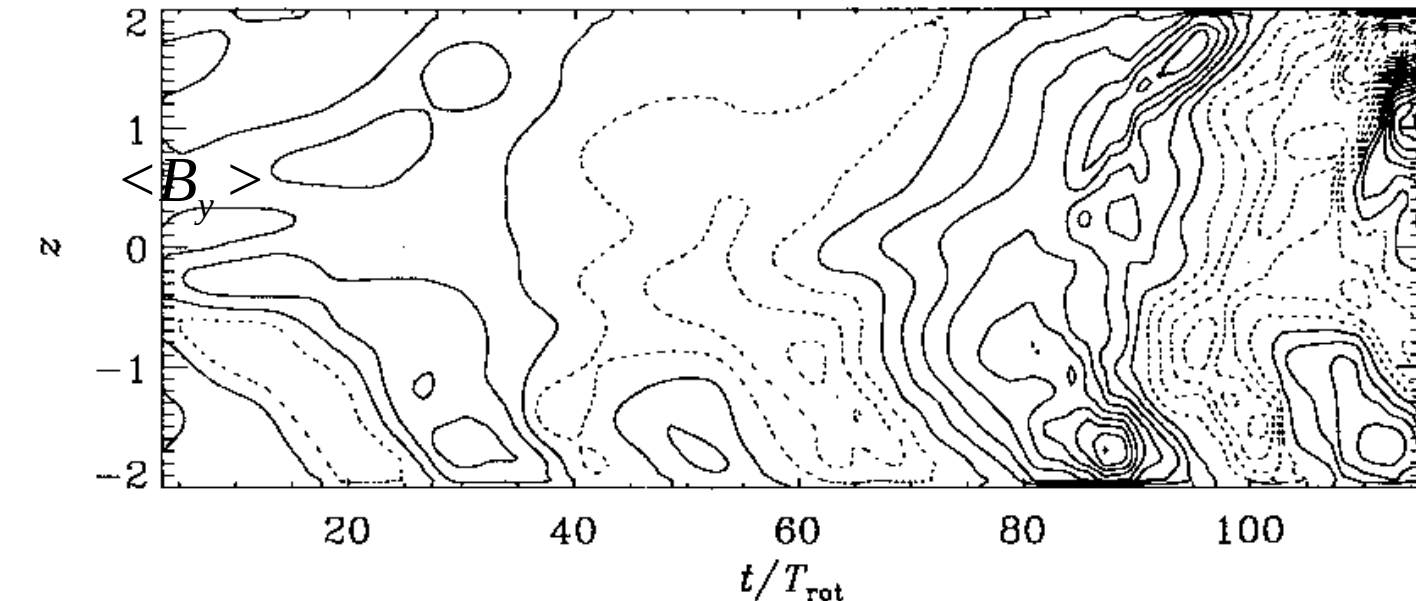


$$\Omega(r) \propto r^{-q}$$

slow
magnetosonic

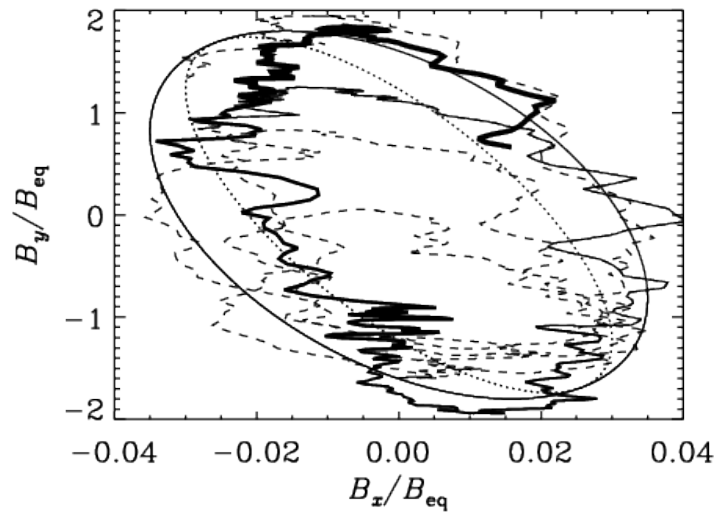
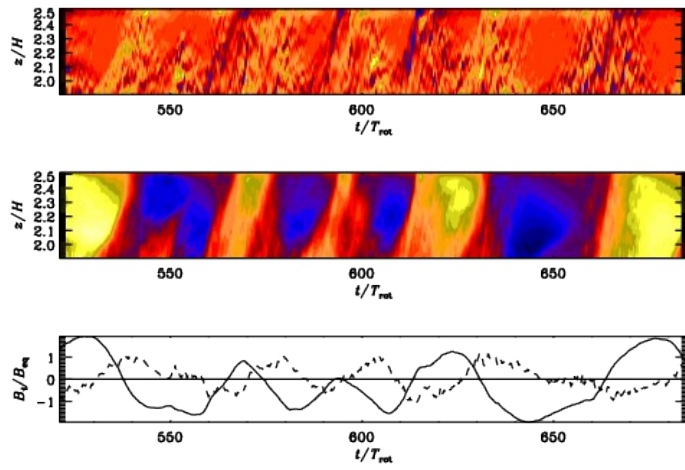
Comparison with stratified runs

Brandenburg et al. (1995)



Dynamo waves
Versus
Buoyant escape

Phase relation in dynamos



Brandenburg et al. (2008)

Mean-field equations:

$$\frac{\partial \bar{B}_x}{\partial t} = -\alpha \frac{\partial \bar{B}_y}{\partial z} + \eta_T \frac{\partial^2 \bar{B}_x}{\partial z^2}$$

$$\frac{\partial \bar{B}_y}{\partial t} = -\frac{3}{2} \Omega \bar{B}_x + \eta_T \frac{\partial^2 \bar{B}_y}{\partial z^2}$$

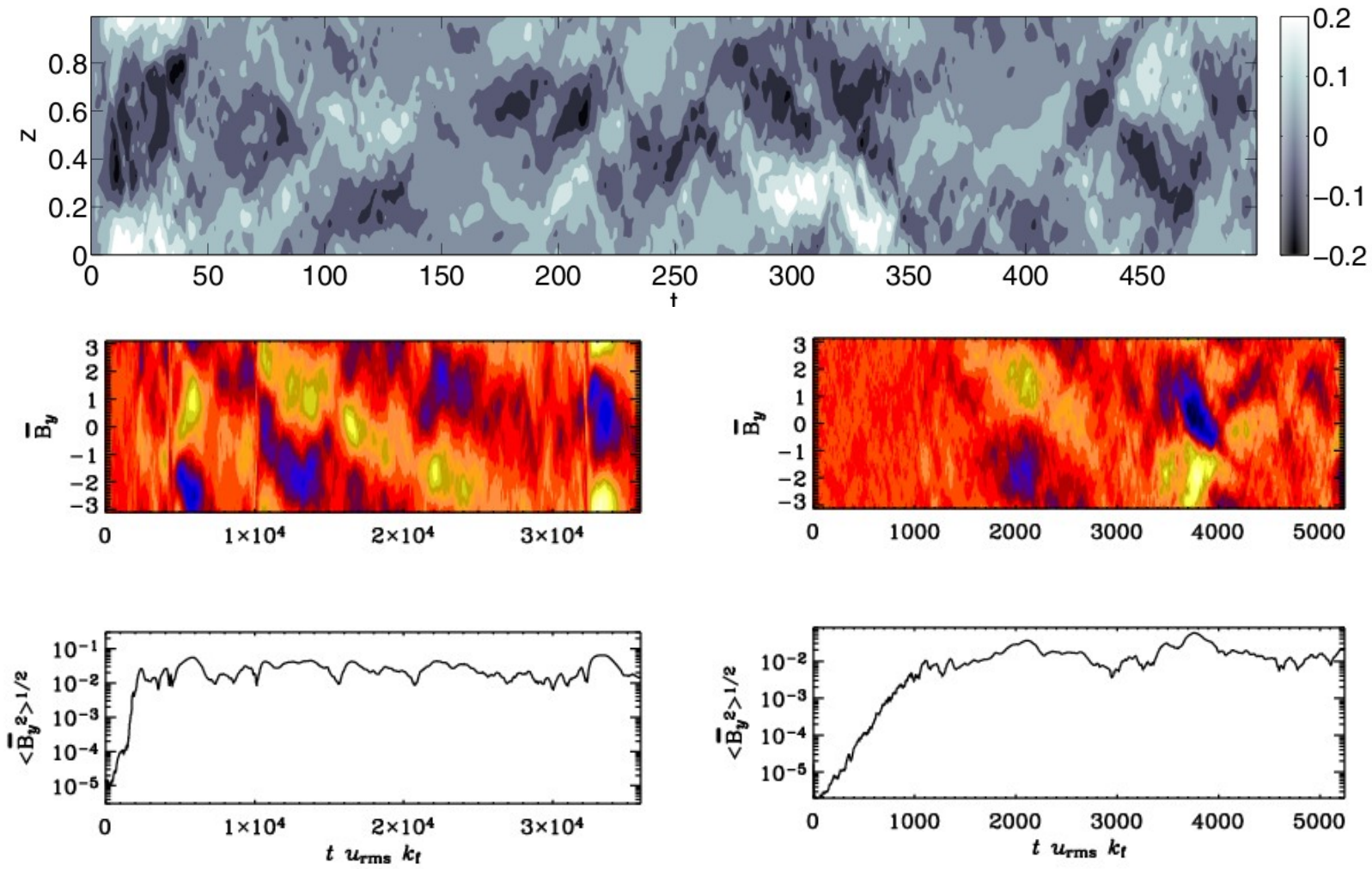
Solution:

$$\bar{B}_x = \sin k(z - ct)$$

$$\bar{B}_y = \sqrt{2} \frac{c}{\alpha} \sin[k(z - ct) \pm \frac{3}{4}\pi]$$

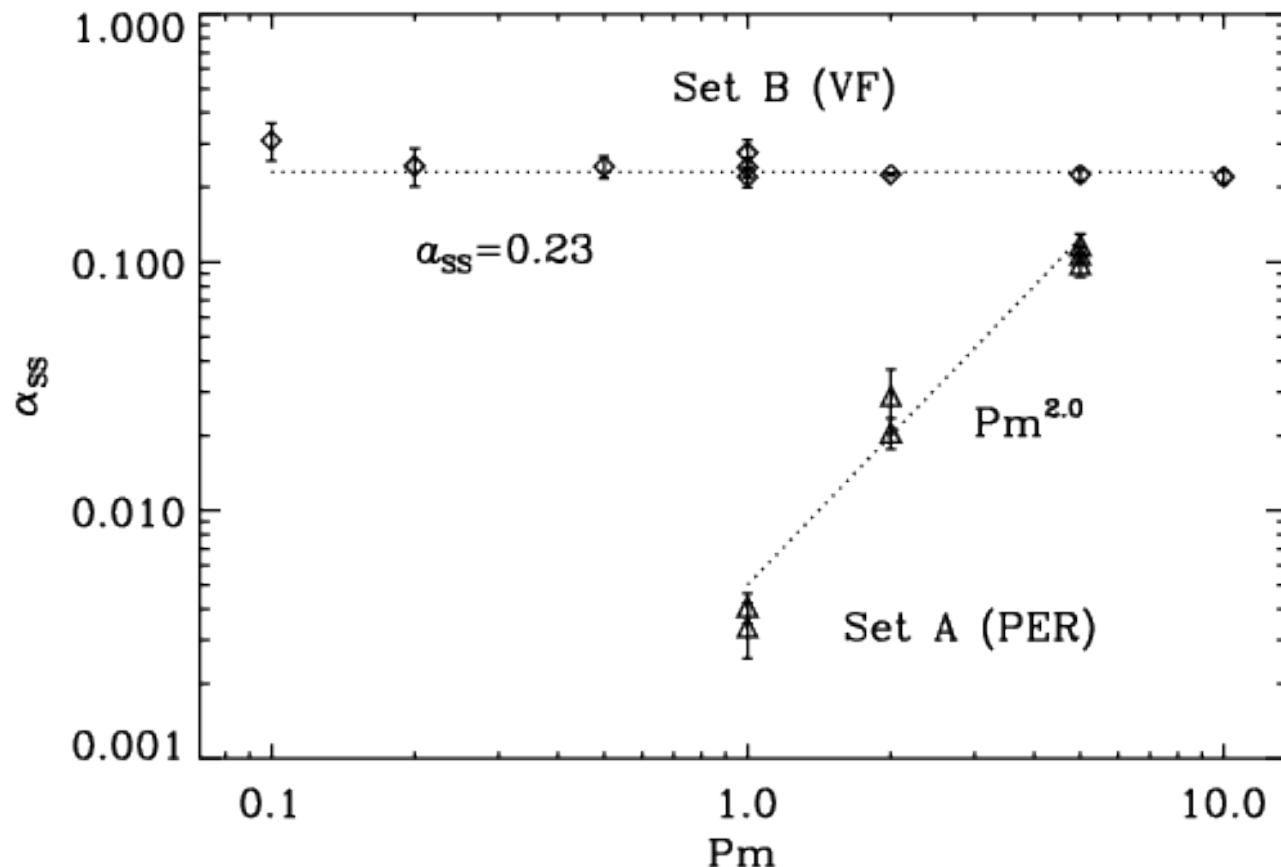
$$c = \frac{\omega}{k} = -\alpha \sqrt{3\Omega / 4\alpha k} = \mp \eta_T k$$

Unstratified: also LS fields?

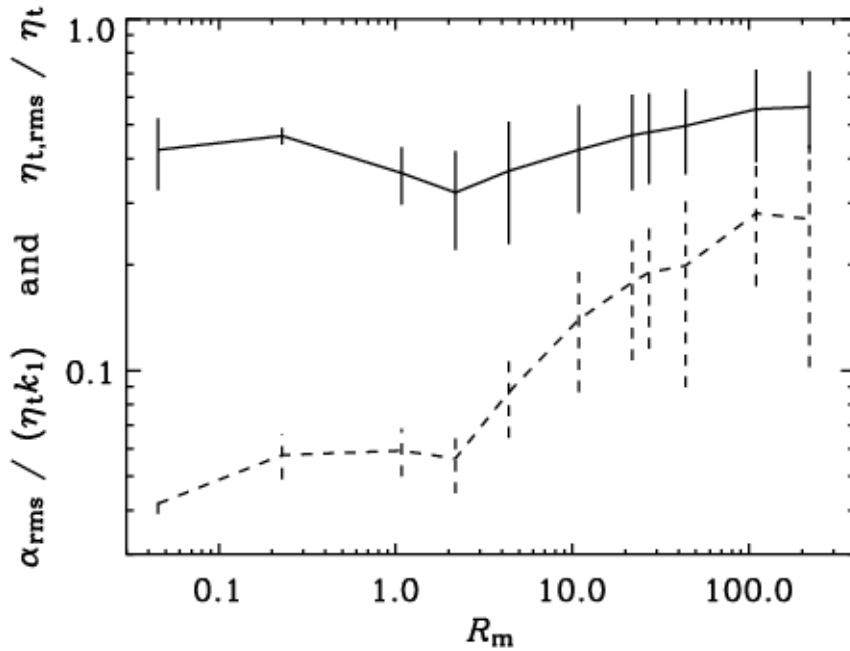


Low Pr_M issue in unstratified MRI

Käpälä & Korpi (2010): vertical field condition

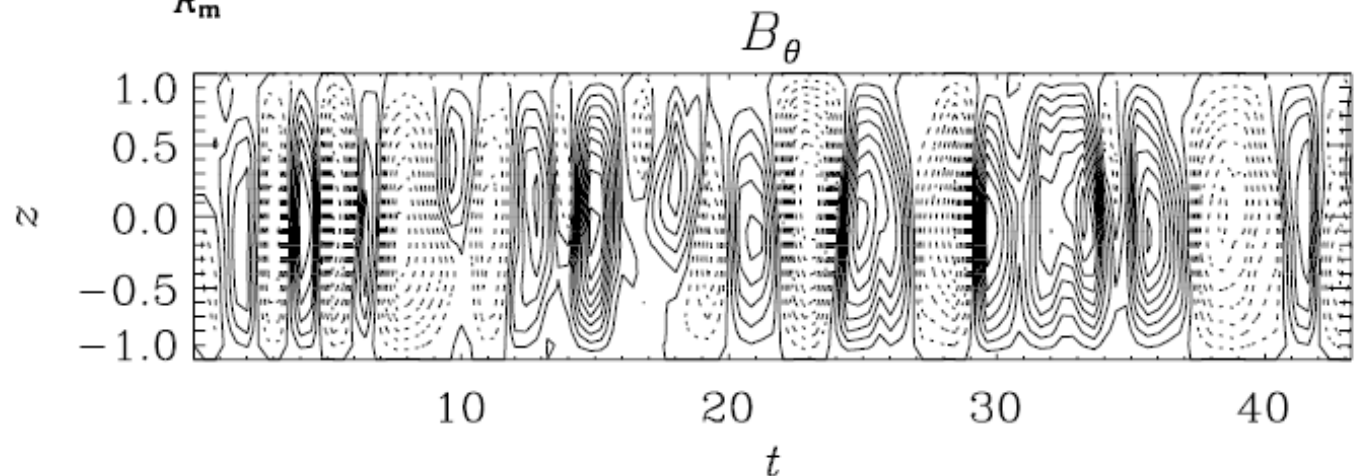


LS from Fluctuations of α_{ij} and η_{ij}



Incoherent α effect
(Vishniac & Brandenburg 1997,
Sokoloff 1997, Silantev 2000,
Proctor 2007)

$$\begin{aligned}\partial_t B_r &= -\partial_z(\alpha B_\theta) + D_t \partial_z^2 B_r , \\ \partial_t B_\theta &= -\frac{3}{2}\Omega B_r + D_t \partial_z^2 B_\theta ,\end{aligned}$$



Magnetic fields in galaxies

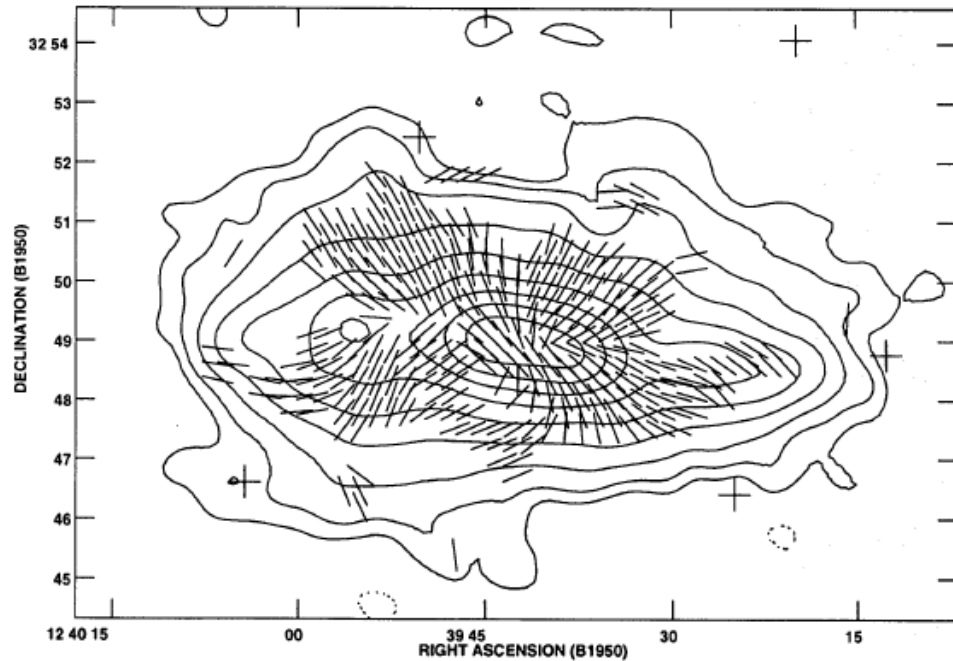
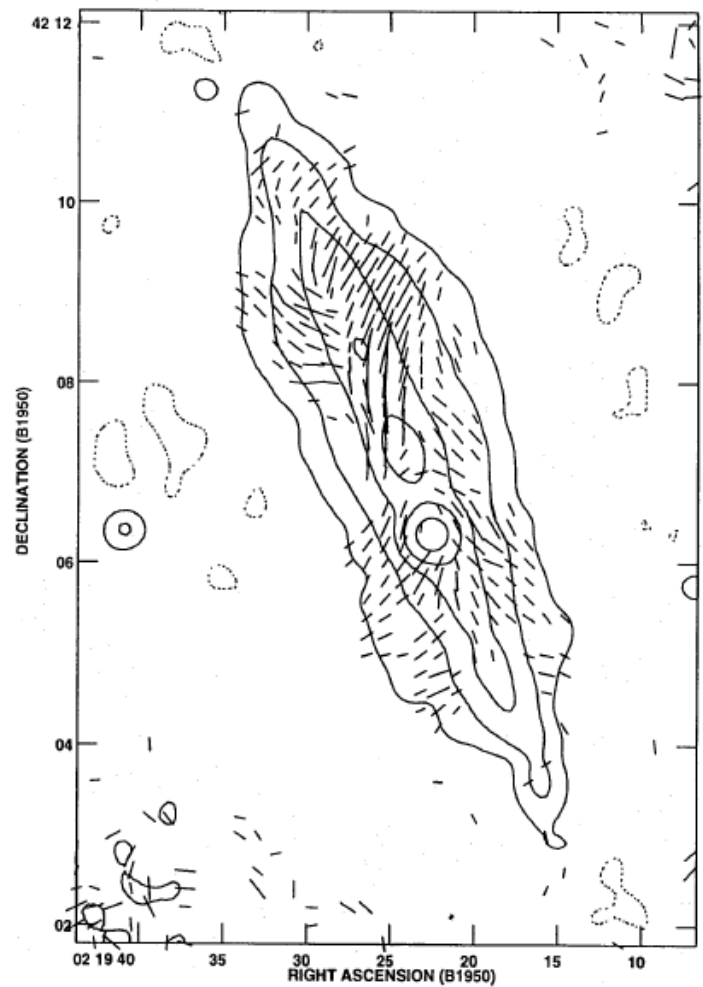


Fig. 1. Total intensity contours with magnetic field orientations indicated by vectors according to observations of NGC 4631 at 6.2 cm by Golla & Hummel (1992). The contours start at 100 mJ/beam and the interval is a factor of 2. The noise in the total intensity map is about $28 \mu\text{J}/\text{beam}$. Vectors are plotted only if the polarised intensity exceeds $\sim 70 \mu\text{J}/\text{beam}$. The half power beam width (HPBW) is $40''$. Assuming a distance of 7.5 Mpc the scale is $1' = 2.2 \text{ kpc}$



Polarized synchrotron emission

Cioffi & Jones (1980)

$$\frac{dI}{dz} = \epsilon$$

$$\frac{dP}{dz} = i f P + p \epsilon$$

P = complex polarization

$$p = p_0 e^{2i\chi}$$

complex polarized emissivity

$$\chi = \pi/2 + \arctan B_y / B_x$$

intrinsic polarization

$$f = 2n_{\text{th}} K B_z \lambda^2$$


R/L

$$K = 0.81 \text{ rad m}^{-2} \text{cm}^3 \mu\text{G}^{-1} \text{pc}^{-1}$$

P = complex polarization

R = intrinsic Faraday rotation measure

Generation and interpretation of galactic magnetic fields

K. J. Donner and A. Brandenburg

Observatory and Astrophysics Laboratory, University of Helsinki, Tähtitorninmäki, SF-00130 Helsinki, Finland

Received April 5; accepted July 31, 1990

The general formulae governing synchrotron emission can be found in e.g. Pacholczyk (1970, Chap. 3 and references therein). For an optically thin source and neglecting circular polarisation the radiation can be described by means of the Stokes parameters I, Q, U governed by the equations

$$\frac{dI}{d\ell} = \epsilon, \quad (7)$$

$$\frac{dQ}{d\ell} = -f \ U - p \ \epsilon \ \cos 2\chi, \quad (8)$$

$$\frac{dU}{d\ell} = f \ Q - p \ \epsilon \ \sin 2\chi, \quad (9)$$

RM around circumference

Generation and interpretation of galactic magnetic fields

K. J. Donner and A. Brandenburg

Observatory and Astrophysics Laboratory, University of Helsinki, Tähtitorninmäki, SF-00130 Helsinki, Finland

Received April 5; accepted July 31, 1990

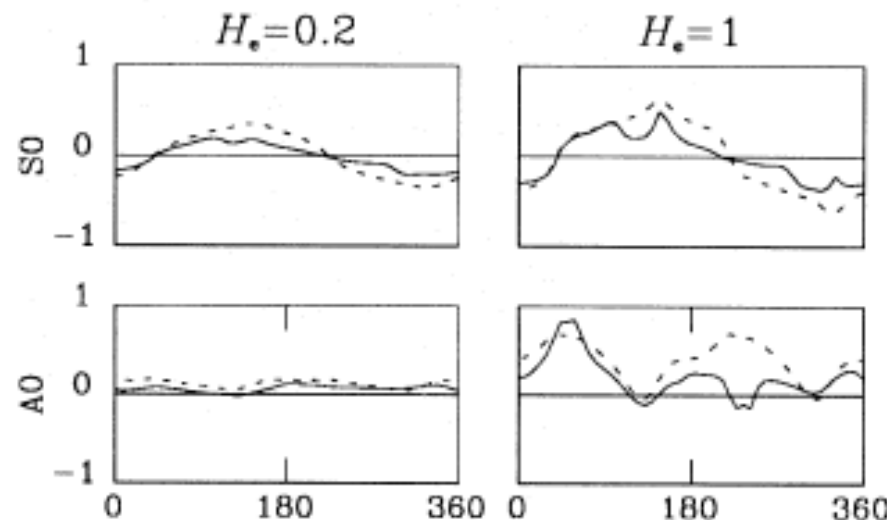
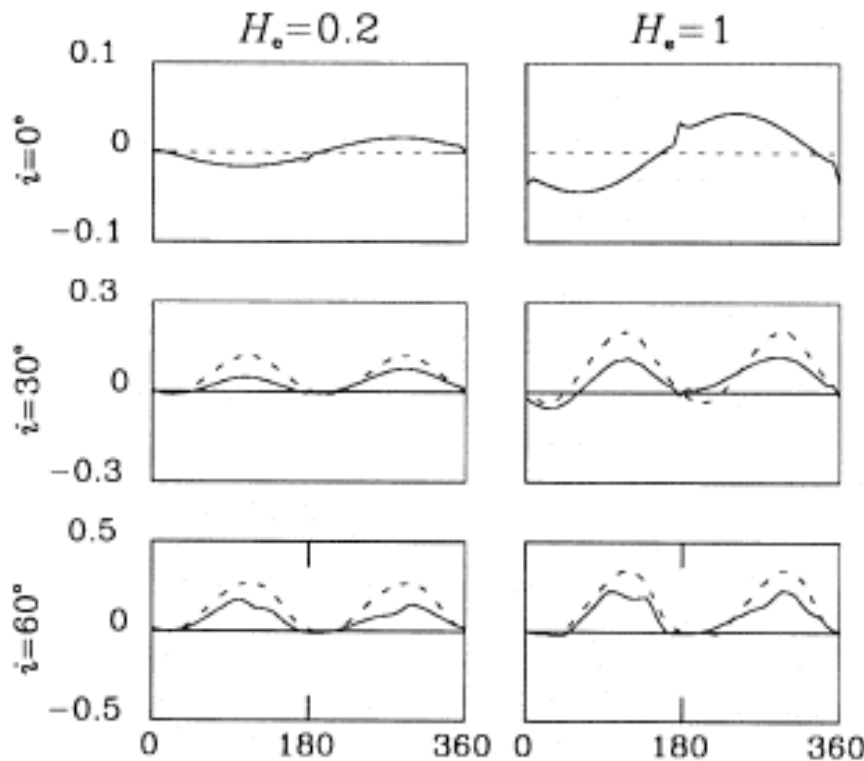


Fig. 12. RM for the S0 and A0 modes for two values of H_c , $i = 60^\circ$. Otherwise the same as Fig. 11.

to emphasise that the variations of RM may be quite complex even in very simple models and that the interpretation of RM observations requires some care.

Polarized synchrotron emission

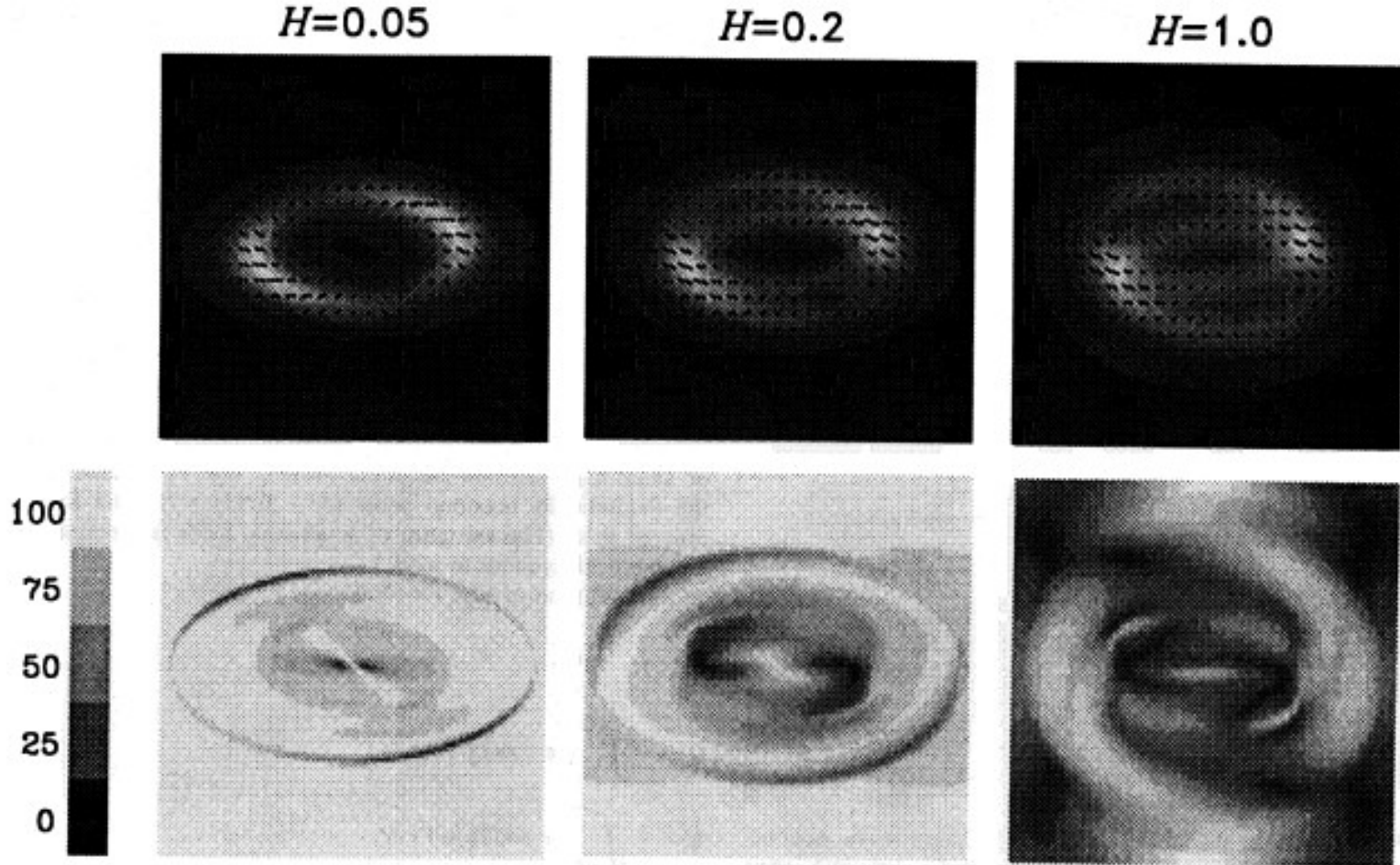
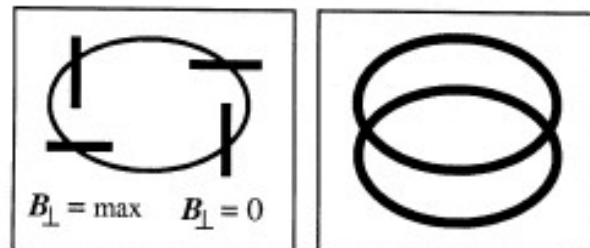


Fig. 6. Synthetical polarisation maps for the S0 mode computed for different values of H_{rel} , $i = 60^\circ$. The upper row is a grey scale representation of the total intensity I . The short lines in this map show the field orientation as inferred from the integrated Stokes parameters. The length of these lines is proportional to the polarised intensity. The lower row gives a grey scale representation of the degree of polarisation relative to its value for a homogeneous field. The strip on the left-hand side gives the calibration of the grey scale in per cent

observes the polarisation angle χ_F at two different wavelengths and determines then the rotation measure $\Delta\chi_F/\Delta\lambda^2$. With this definition of the rotation measure we obtain

$$\text{RM} = (Q_1 U_0 - U_1 Q_0)/(Q_0^2 + U_0^2), \quad (22)$$

which can be computed from (18)-(21).



Integrating factor

Integrating factor

$$\frac{dP}{dz} = ifP + p\varepsilon$$

$$e^{-iF} \frac{d}{dz} P e^{iF} = p\varepsilon \quad \frac{dF}{dz} = -f$$

Equation to be integrated

$$\frac{dP}{dz} = p_0\varepsilon e^{2i(\chi+\phi\lambda^2)} \quad 2\phi\lambda^2 = F$$

$\square(z)$ = Faraday depth

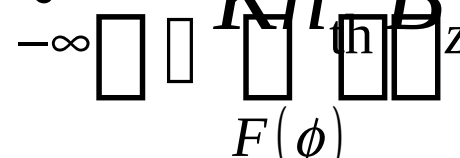
$$P = Q + iU$$

Faraday space

$$P = p_0 \int_{-\infty}^{\infty} \varepsilon e^{2i(\chi + \phi\lambda^2)} dz$$

$$P = p_0 \int_{-\infty}^{\infty} \frac{dz}{d\phi} \varepsilon e^{2i(\chi + \phi\lambda^2)} d\phi$$

$$P(\lambda^2) = \int_{-\infty}^{\infty} p_0 \frac{\varepsilon e^{2i\chi}}{Kn_B F(\phi)} e^{2i\phi\lambda^2} d\phi$$



→ 38

Stationary phase

Helical perpendicular fields with pos and neg helicity

$$B = \begin{pmatrix} B_1 \sin kz \\ B_1 \cos kz \\ B_0 \end{pmatrix} \quad B = \begin{pmatrix} B_1 \cos kz \\ B_1 \sin kz \\ B_0 \end{pmatrix}$$

Integration

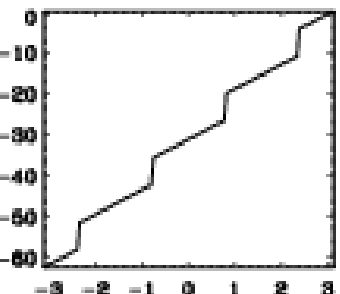
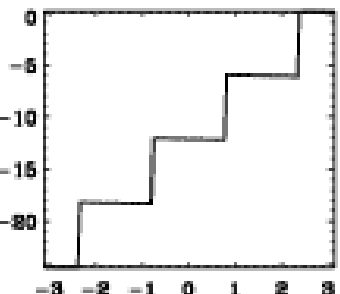
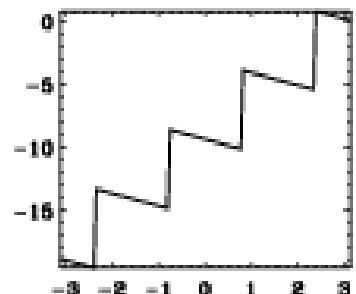
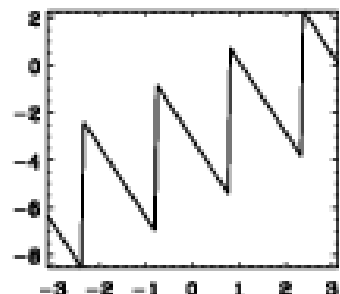
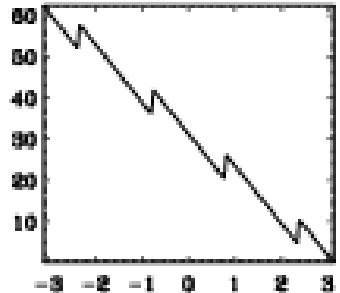
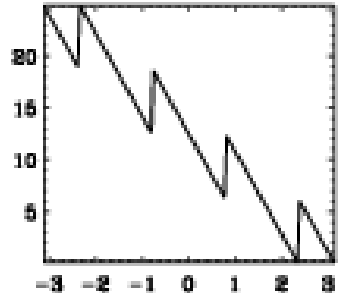
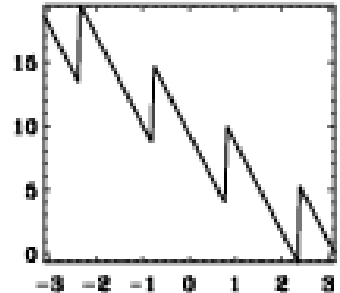
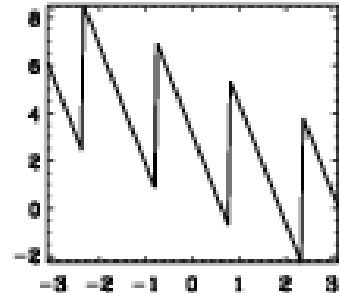
$$Q = p_0 \int_{-\infty}^{\infty} \varepsilon \cos 2(\chi + \phi \lambda^2) dz \quad \phi = K n_{\text{th}} B_0 z$$

$$U = p_0 \int_{-\infty}^{\infty} \varepsilon \sin 2(\chi + \phi \lambda^2) dz$$

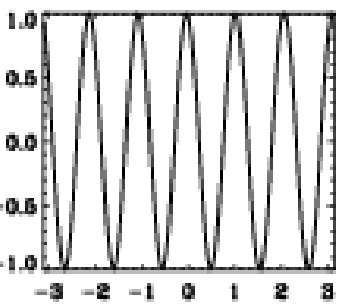
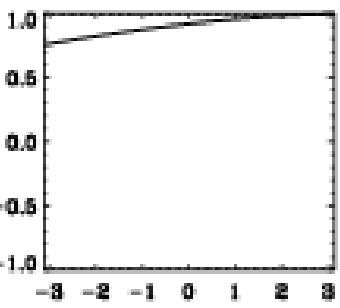
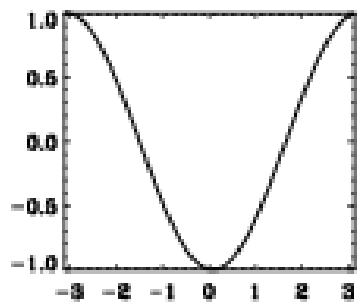
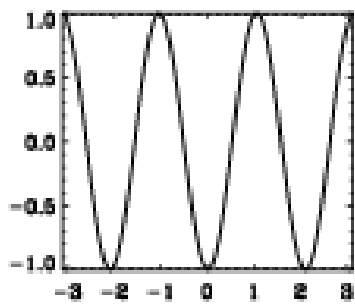
Stationary:

$$Q = p_0 \int_{-\infty}^{\infty} \varepsilon \cos 2(\chi + \phi \lambda^2) dz$$

$$2(\chi + \phi \lambda^2)$$



$$\cos 2(\chi + \phi \lambda^2)$$



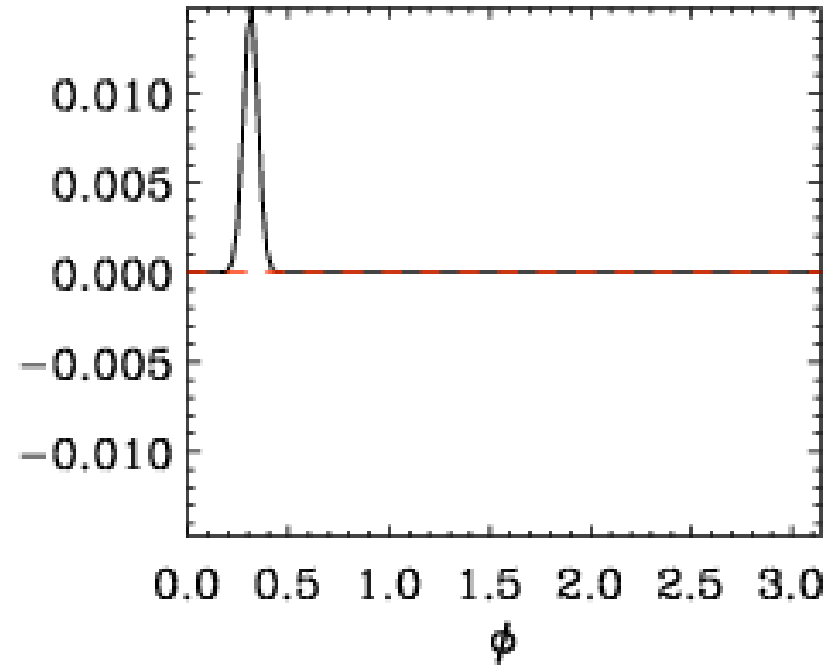
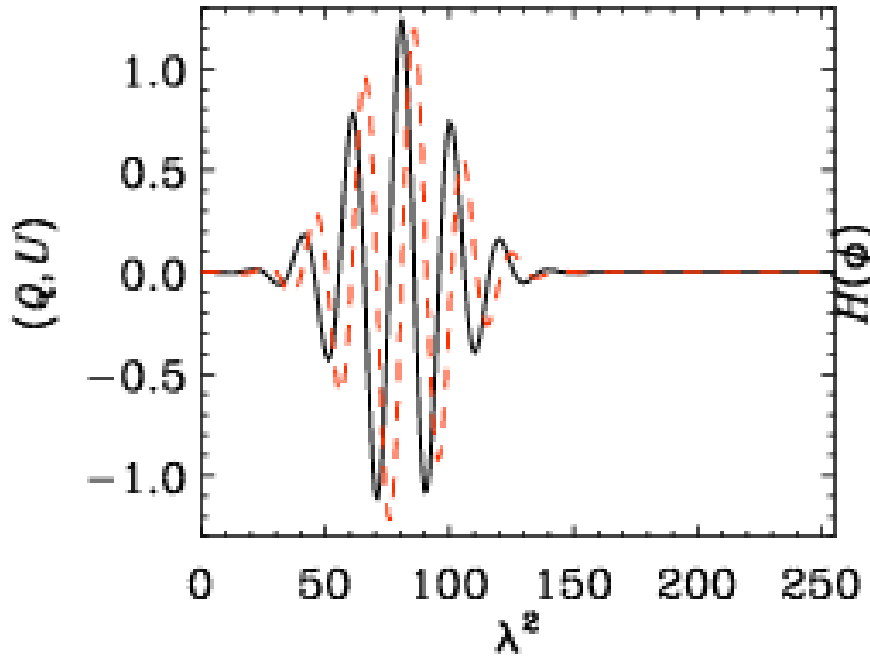
Positive helicity as input

$$\hat{Q}(\phi) = \int_{\lambda_{\min}^2}^{\lambda_{\max}^2} Q(\lambda^2) e^{2i\phi\lambda^2} d\lambda^2$$

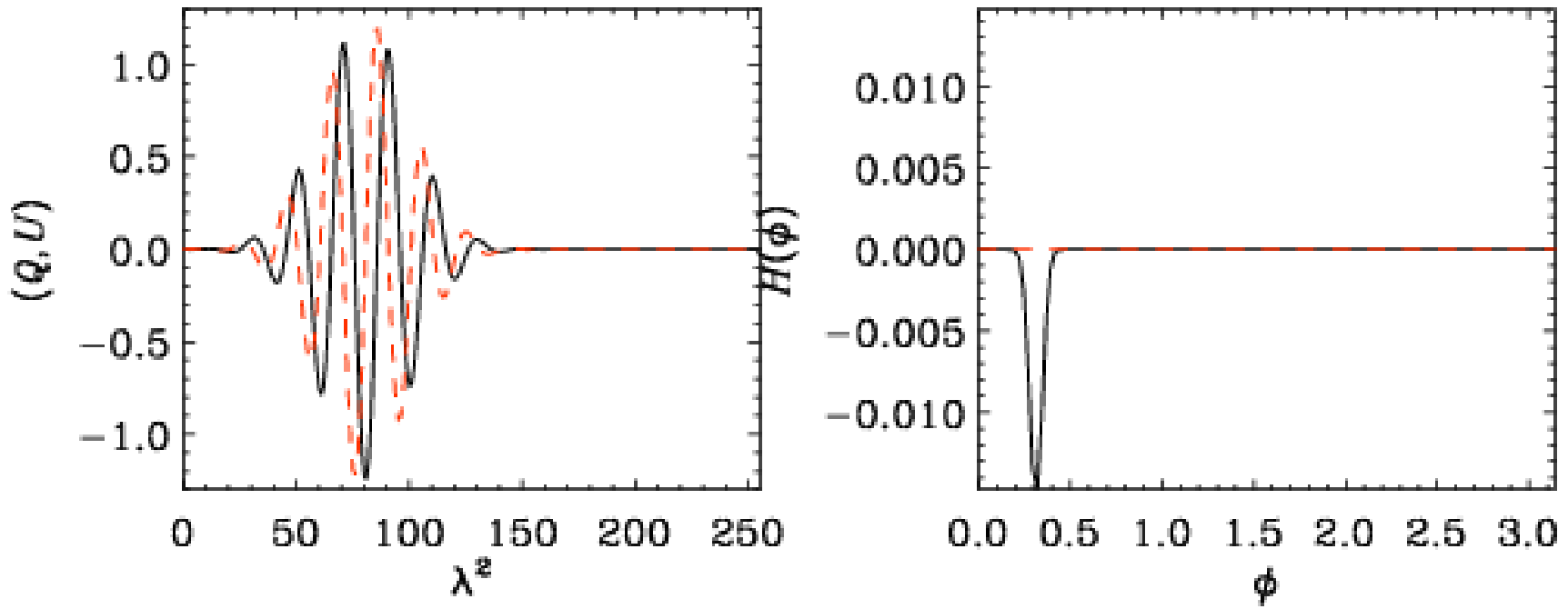
$$H(\phi) = \text{Im}(\hat{Q}\hat{U}^*)$$

$$\hat{U}(\phi) = \int_{\lambda_{\min}^2}^{\lambda_{\max}^2} U(\lambda^2) e^{2i\phi\lambda^2} d\lambda^2$$

Why? By analogy; just try



Negative helicity as input



Helicity proxy also reversed in sign!

Dynamo effect in SNR

$$\rho \frac{\partial \mathbf{U}}{\partial t} = -\nabla P + \frac{1}{c} \mathbf{J} \times \mathbf{B} + e(n_i - n_e) \mathbf{E} + \mathbf{F}_v$$

$$\nabla \times \mathbf{B} = \frac{4\pi}{c} (\mathbf{J} + \mathbf{J}_{\text{cr}}) \quad n_i + n_{cr} = n_e$$

$$\rho \frac{\partial \mathbf{U}}{\partial t} = -\nabla P + \left(\frac{1}{4\pi} \nabla \times \mathbf{B} - \frac{1}{c} \mathbf{J}_{\text{cr}} \right) \times \mathbf{B} + e n_{\text{cr}} \mathbf{U} \times \mathbf{B} + \mathbf{F}_v$$

To be solved with induction equation
and continuity equation, isothermal EOS

Introduces pseudoscalar: helicity

$\Omega \cdot g \rightarrow \alpha$ effect in stars

$$\mathbf{J}_{\text{cr}} \cdot \mathbf{B}_0 \rightarrow \alpha \text{ effect}$$

α effect important for large-scale field in the Sun

$$\frac{\partial \bar{\mathbf{B}}}{\partial t} = \nabla \times (\bar{\mathbf{U}} \times \bar{\mathbf{B}} + \bar{\mathbf{u}} \times \bar{\mathbf{b}} - \bar{\mathbf{J}} / \sigma)$$

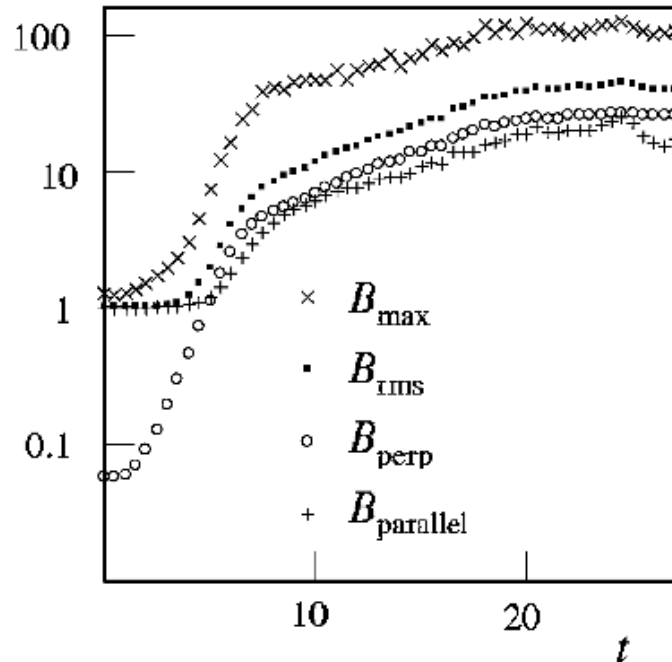


$$\bar{\mathbf{E}} \equiv \bar{\mathbf{u}} \times \bar{\mathbf{b}} = \alpha \bar{\mathbf{B}} + \dots$$

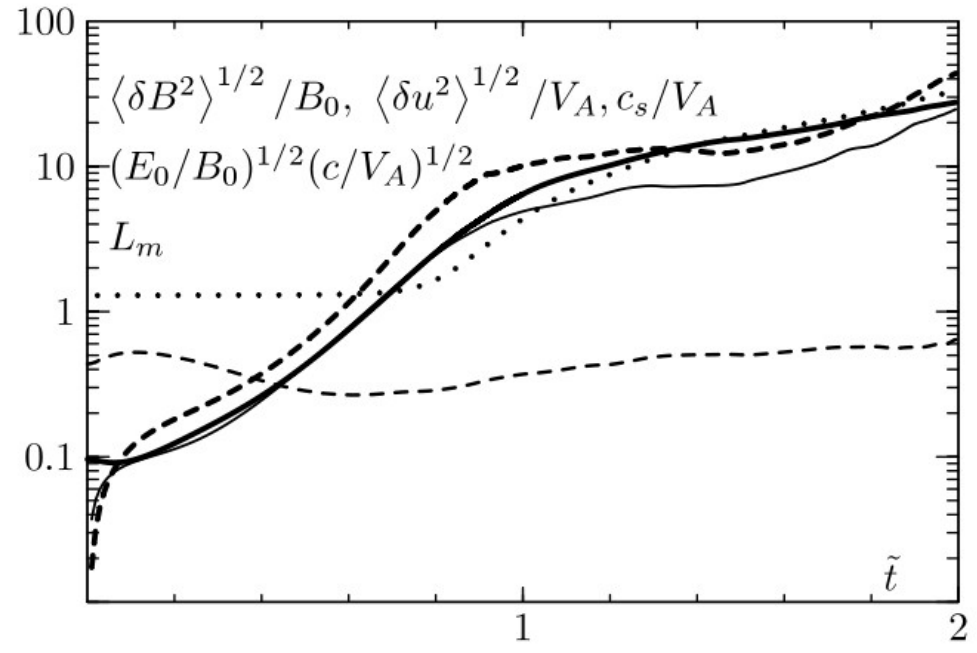
$$\bar{\mathbf{E}}_i = \alpha_{ij} \bar{B}_j - \eta_{ij} \bar{J}_j + \dots$$

Bell instability

$$\gamma_B^2 = \left(\frac{4\pi}{c} \frac{J_{\text{cr}}}{B} k_z - k^2 \right) v_A^2 \quad J = \frac{4\pi}{c} J_{\text{cr}} / kB_0$$



Bell (2004): $J=2$



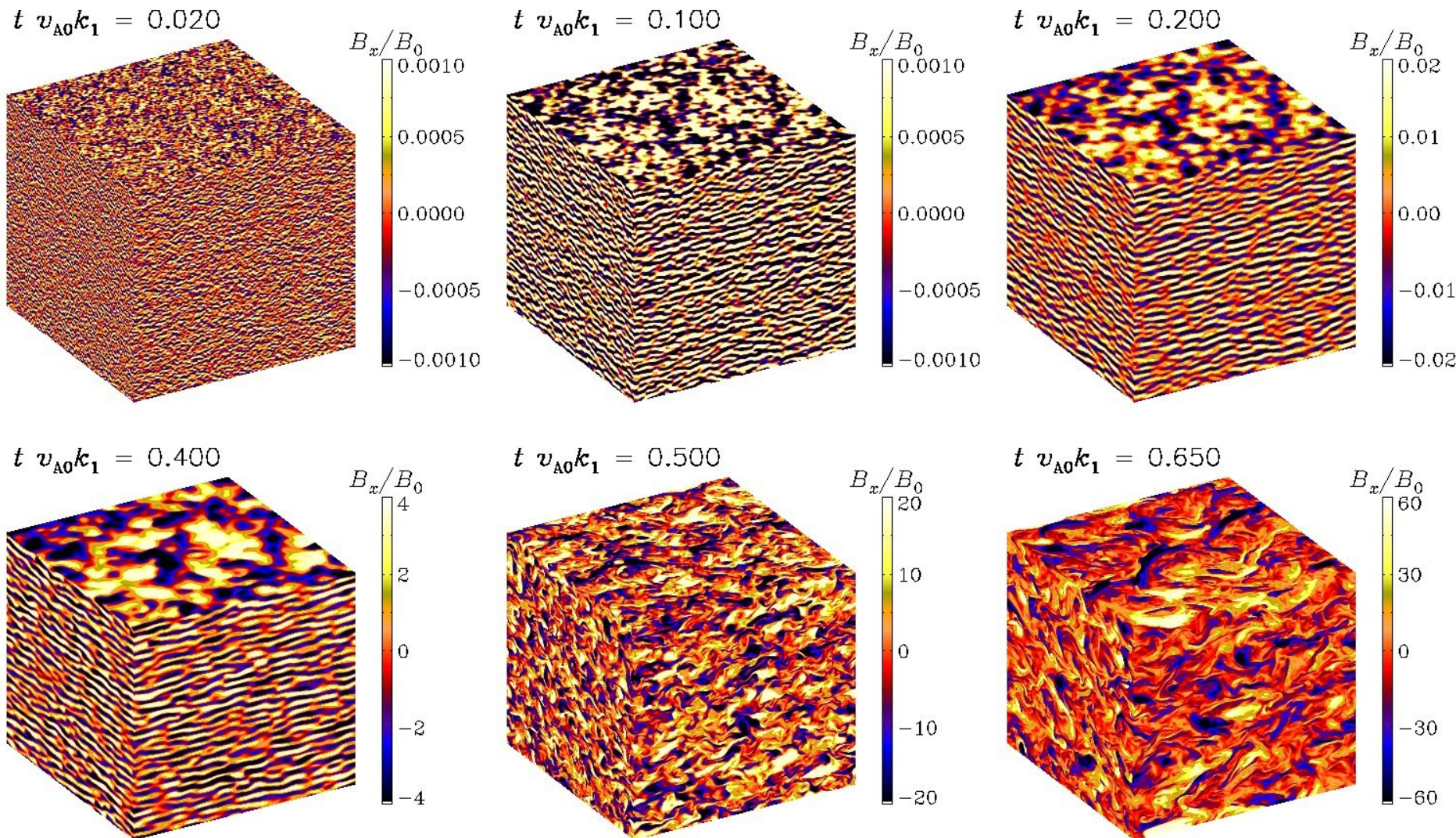
Zirakashvili et al (2008): $J=16$

Continued growth in both cases! $\rightarrow \alpha$ effect important?

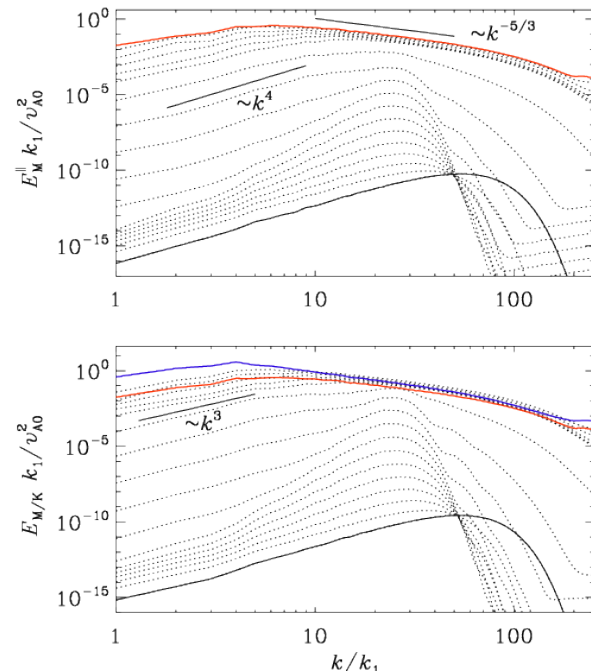
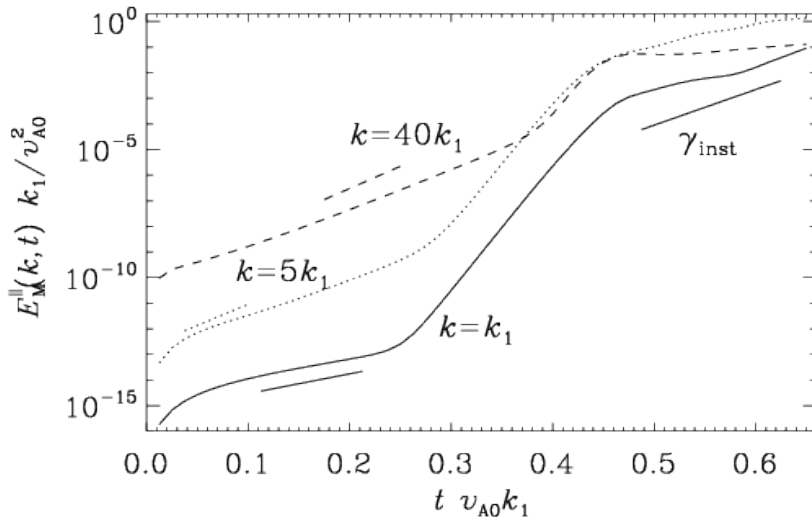
New simulations

- 512^3 resolution, non-ideal ($\text{Re}=\text{Lu} < 300$)
- larger J parameter (80 and 800)
- most unstable $k / k_1 = 40$ and 400 (unresolved)
- measure alpha and turbulent diff. tensor
- Related to earlier work by Bykov et al. (2011)

Bell instability → turbulence ($\beta=80$)

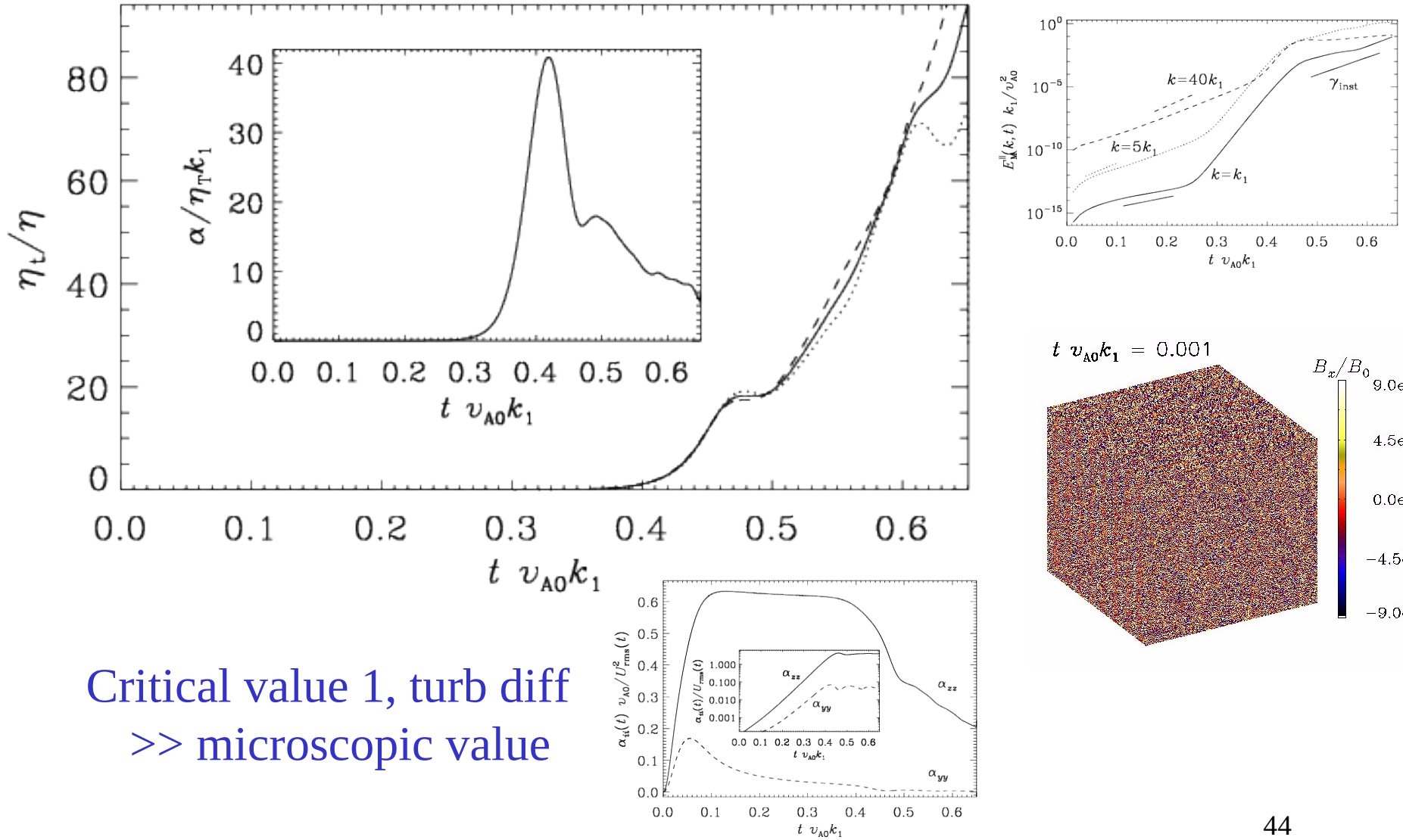


3 stages

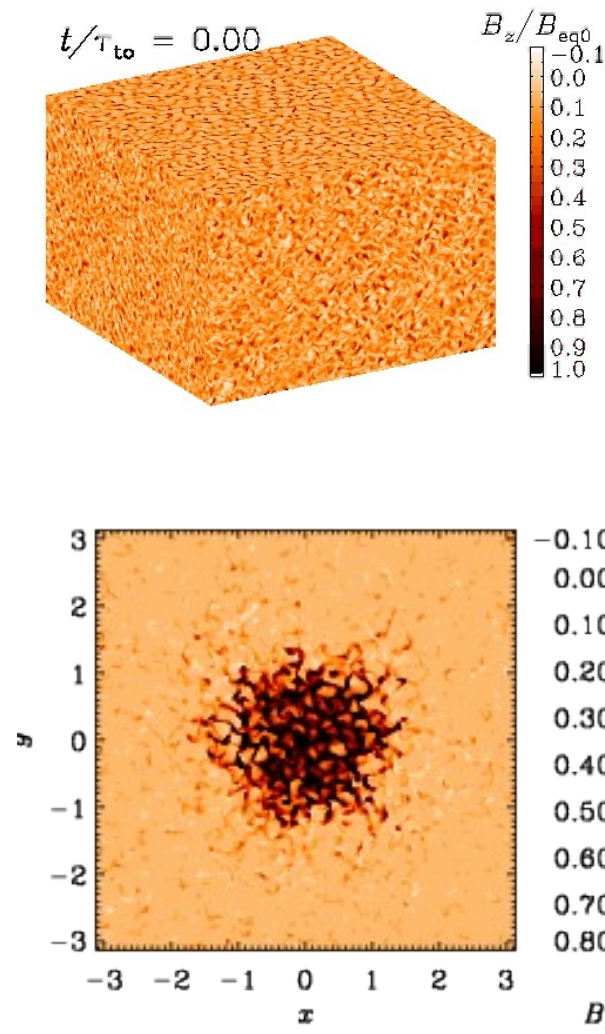
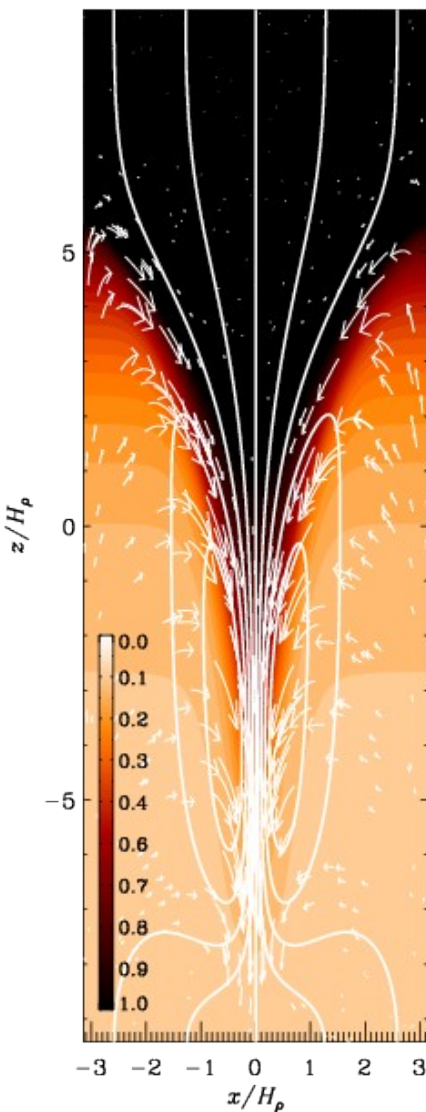


- Bell instability, small scale, $k/k_1=40$
- Accelerated large-scale growth
- Slow growth after initial saturation

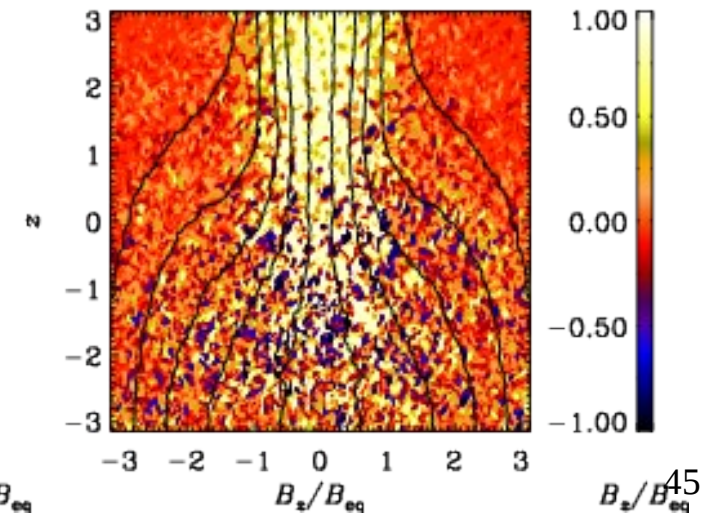
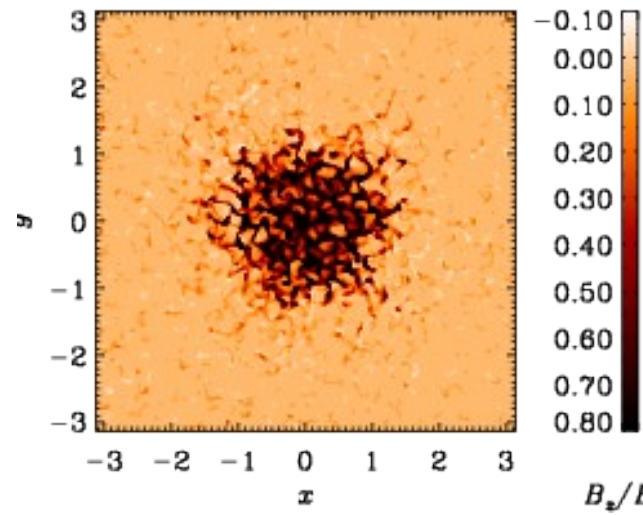
Dynamo number, turb diff



New theory for magnetic spots



- Minimalistic model
- 2 ingredients:
 - Stratification & turbulence
- Extensions
 - Coupled to dynamo
 - Compete with rotation
 - Radiation/ionization



45

Conclusions

- Spherical dynamos
 - Equatorward migration
 - TFM
- Low PrM issue
- MRI dynamos
 - Phase relation
- Galactic dynamos
 - RM synthesis
- Bell-dynamo instability

